NICA

Nuclotron-based
Ion Collider fAcility

First physics for the MPD

V. Riabov for the MPD Collaboration

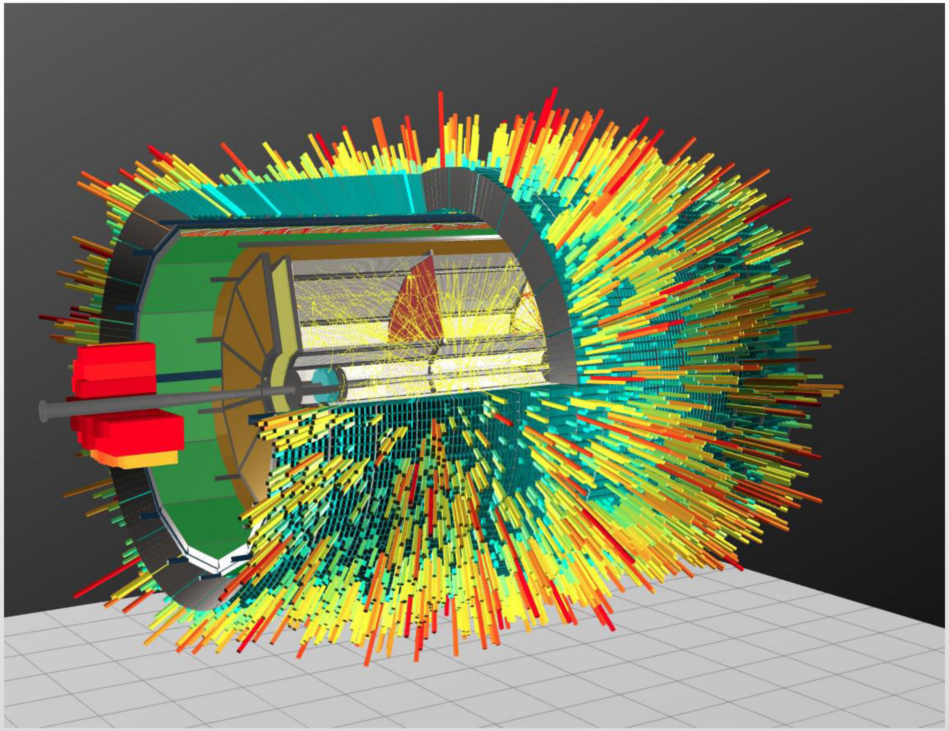

Heavy-ion collisions

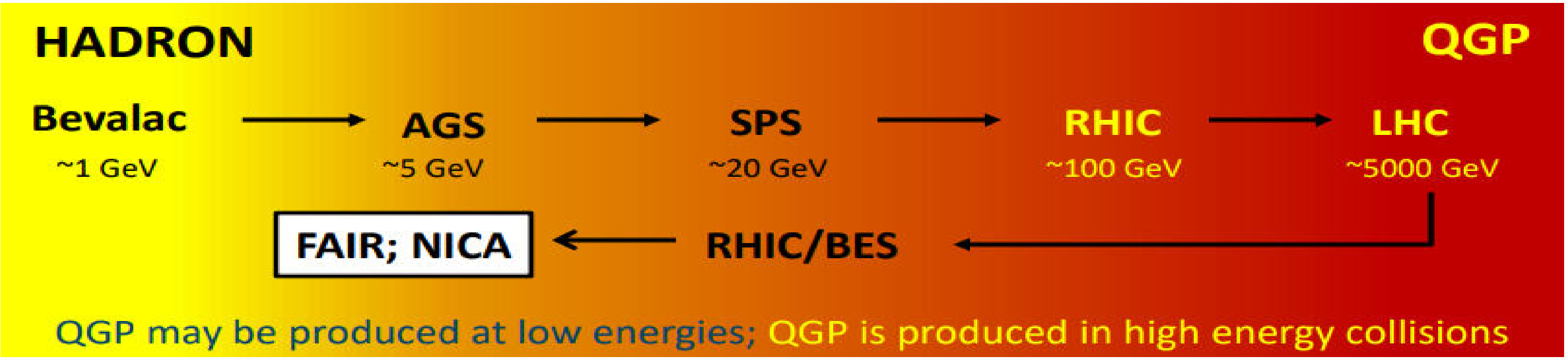

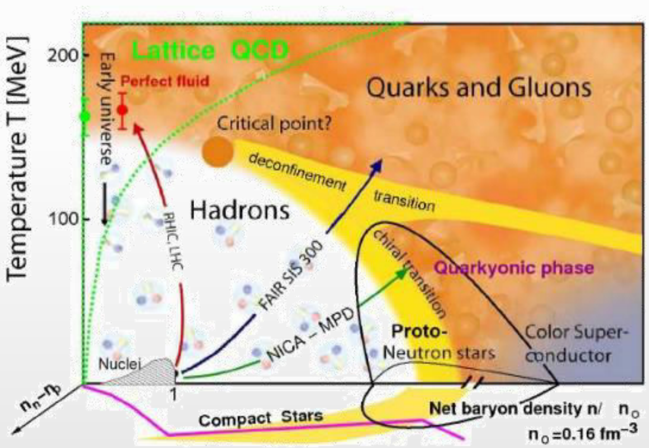

High beam energies ($\sqrt{s_{NN}}$ > 100 GeV)

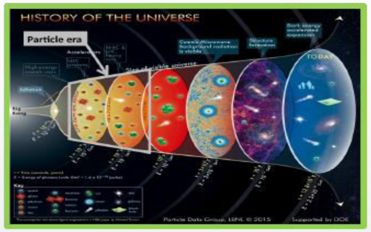

High temperature:
Early Universe evolution

Low beam energies ($\sqrt{s_{NN}}$~ 10 GeV)

High baryon density:
Inner structure of
compact stars

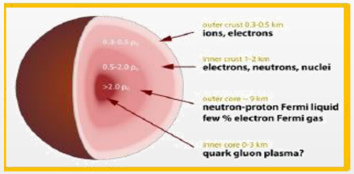

- At μ_B ~ 0, smooth crossover (lattice QCD calculations + data)
- At large μ_B, 1st order phase transition is expected → QCD critical point
- At NICA, both BM@N and MPD study QCD medium at extreme net baryon densities

Fixed-target operation at NICA

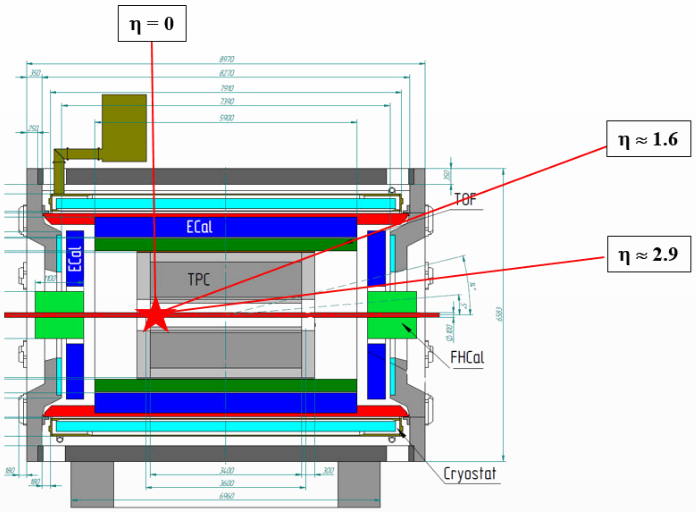

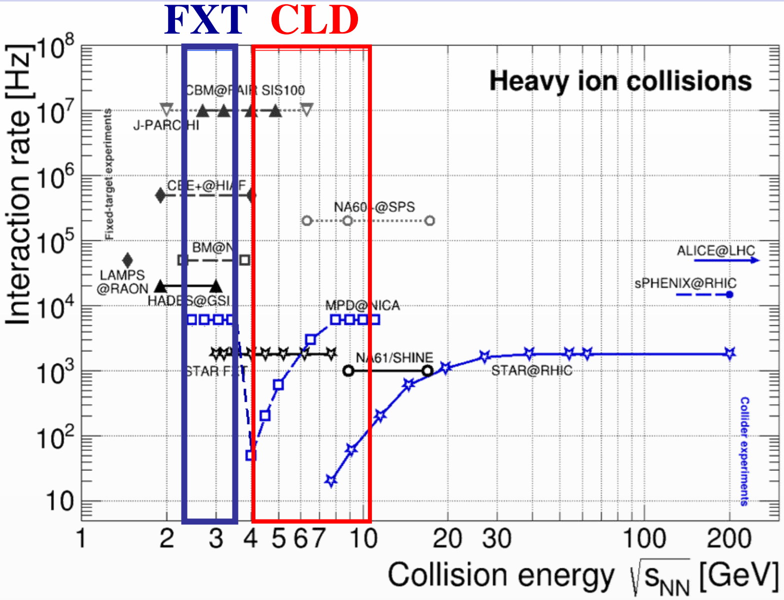

- MPD-CLD and MPD-FXT options approved by accelerator department (default option from start-up)
- Collider mode: two beams, $\sqrt{s_{NN}}$ = 4-11 GeV
- Fixed-target mode: one beam + thin wire (~ 50-100 μm) close to the edge of the MPD central barrel:
  - ✓ extends energy range of MPD to $\sqrt{s_{NN}}$ = 2.4-3.5 GeV (overlap with HADES, BM@N and CBM)
  - ✓ solves problem of low event rate at lower collision energies (only ~ 50 Hz at $\sqrt{s_{NN}}$ = 4 GeV at design luminosity)
- Expected beam condition for the first year(s):
  - ✓ MPD-CLD: Xe+Xe/Bi+Bi at $\sqrt{s_{NN}}$ ~ 7 GeV, reduced luminosity → collision rate ~ 50 Hz
  - ✓ MPD-FXT: Xe/Bi+W at $\sqrt{s_{NN}}$ ~ 3 GeV

Capability of target and collision energy overlap between MPD and BM@N experiments

Multi-Purpose Detector (MPD) Collaboration

MPD** International Collaboration was established in **2018
to construct, commission and operate the detector

12** Countries, **>500** participants, **38** Institutes and **JINR

Organization

Acting Spokesperson:	***Victor Riabov***
Deputy Spokespersons:	***Zebo Tang, Arkadiy Taranenko***
Institutional Board Chair:	***Alejandro Ayala***
Project Manager:	***Slava Golovatyuk***

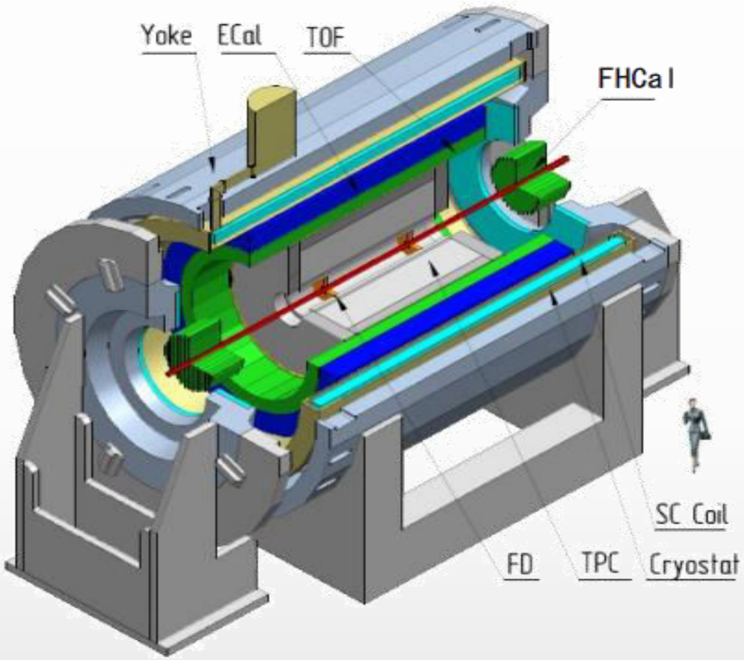

***Joint Institute for Nuclear Research, Dubna**;*
*A.Alikhanyan National Lab of Armenia, Yerevan, **Armenia;***
*SSI "Joint Institute for Energy and Nuclear Research – Sosny" of the National Academy of Sciences of Belarus, Minsk, **Belarus***
*University of Plovdiv, **Bulgaria;***
*Tsinghua University, Beijing, **China**;*
*University of Science and Technology of China, Hefei, **China**;*
*Huzhou University, Huzhou, **China**;*
*Institute of Nuclear and Applied Physics, CAS, Shanghai, **China**;*
*Central China Normal University, **China**;*
*Shandong University, Shandong, **China**;*
*University of Chinese Academy of Sciences, Beijing, **China**;*
*University of South China, **China**;*
*Three Gorges University, **China**;*
*Institute of Modern Physics of CAS, Lanzhou, **China**;*
*Tbilisi State University, Tbilisi, **Georgia**;*
*Institute of Physics and Technology, Almaty, **Kazakhstan**;*
*Benemérita Universidad Autónoma de Puebla, **Mexico**;*
*Centro de Investigación y de Estudios Avanzados, **Mexico**;*
*Instituto de Ciencias Nucleares, UNAM, **Mexico**;*
*Universidad Autónoma de Sinaloa, **Mexico**;*
*Universidad de Colima, **Mexico**;*
*Universidad de Sonora, **Mexico**;*
*Universidad Michoacana de San Nicolás de Hidalgo, **Mexico***
*Institute of Applied Physics, Chisinev, **Moldova**;*
*Institute of Physics and Technology, **Mongolia**;*

*Belgorod National Research University, **Russia**;*
*Institute for Nuclear Research of the RAS, Moscow, **Russia**;*
*High School of Economics University, Moscow, **Russia***
*National Research Nuclear University MEPhI , Moscow, **Russia**;*
*Moscow Institute of Science and Technology, **Russia**;*
*North Osetian State University, **Russia**;*
*National Research Center "Kurchatov Institute", **Russia**;*
*Peter the Great St. Petersburg Polytechnic University Saint Petersburg, **Russia**;*
*Plekhanov Russian University of Economics, Moscow, **Russia**;*
*St.Petersburg State University, **Russia**;*
*Skobeltsyn Institute of Nuclear Physics, Moscow, **Russia**;*
*Petersburg Nuclear Physics Institute, Gatchina**, Russia**;*
*Vinča Institute of Nuclear Sciences**, Serbia**;*
*Pavol Jozef Šafárik University, Košice, **Slovakia***

MPD strategy

- ❖ MPD strategy – high-luminosity scans in **energy** and **system size** to measure a wide variety of signals:
  - ✓ order of the phase transition and search for the QCD critical point → structure of the QCD phase diagram
  - ✓ hypernuclei and equation of state at high baryon densities → inner structure of compact stars, star mergers
- ❖ Scans to be carried out using the **same apparatus** with all the advantages of collider experiments:
  - ✓ maximum phase space, minimally biased acceptance, free of target parasitic effects
  - ✓ correlated systematic effects for different systems and energies → simplified extraction of physical signals

Status and initial physics performance studies of the MPD experiment at NICA

MPD Collaboration @ Eur.Phys.J.A 58 (2022) 7, 140 (~ 50 pages)

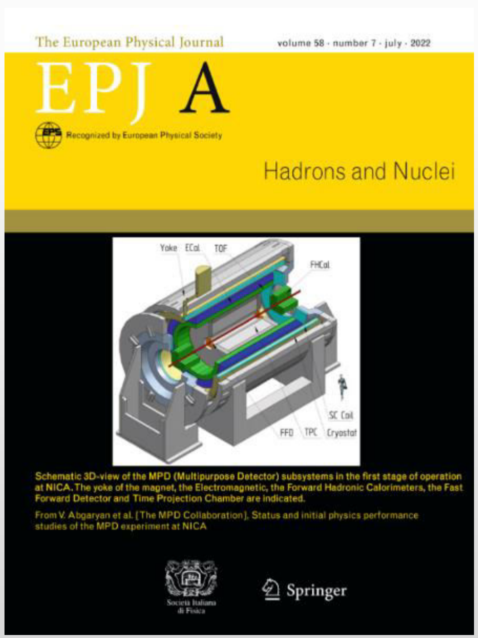

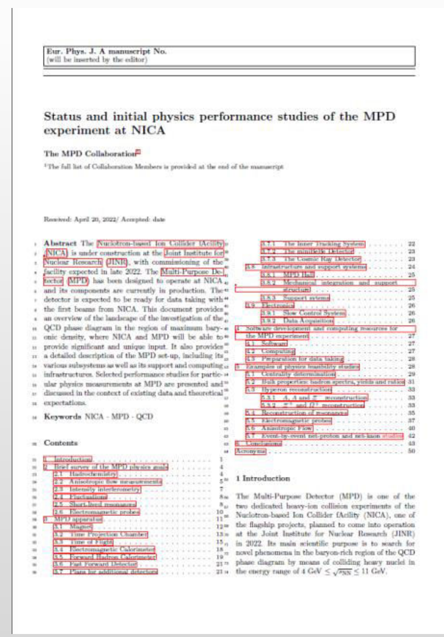
Eur. Phys. J. A manuscript No.
(will be inserted by the editor)

Status and initial physics performance studies of the MPD experiment at NICA

The MPD Collaboration

Contents

1 Introduction

MPD physics program

G. Feofilov, P. Parfenov

Global observables
- Total event multiplicity
- Total event energy
- Centrality determination
- Total cross-section measurement
- Event plane measurement at all rapidities
- Spectator measurement

V. Kolesnikov, Xianglei Zhu

Spectra of light flavor and hypernuclei
- Light flavor spectra
- Hyperons and hypernuclei
- Total particle yields and yield ratios
- Kinematic and chemical properties of the event
- Mapping QCD Phase Diag.

K. Mikhailov, A. Taranenko

Correlations and Fluctuations
- Collective flow for hadrons
- Vorticity, Λ polarization
- E-by-E fluctuation of multiplicity, momentum and conserved quantities
- Femtoscopy
- Forward-Backward corr.
- Jet-like correlations

D. Peresunko, Chi Yang

Electromagnetic probes
- Electromagnetic calorimeter meas.
- Photons in ECAL and central barrel
- Low mass dilepton spectra in-medium modification of resonances and intermediate mass region

Wangmei Zha, A. Zinchenko

Heavy flavor
- Study of open charm production
- Charmonium with ECAL and central barrel
- Charmed meson through secondary vertices in ITS and HF electrons
- Explore production at charm threshold

Physics feasibility studies

- Physics feasibility studies using centralized large-scale MC productions (~ 100M events)
- Centralized Analysis Framework for access and analysis of data → Analysis Train:
  - ✓ consistent approaches and results across collaboration, easy storage and sharing of codes
  - ✓ reduced number of input/output operations for disks and databases, easier data storage on tapes

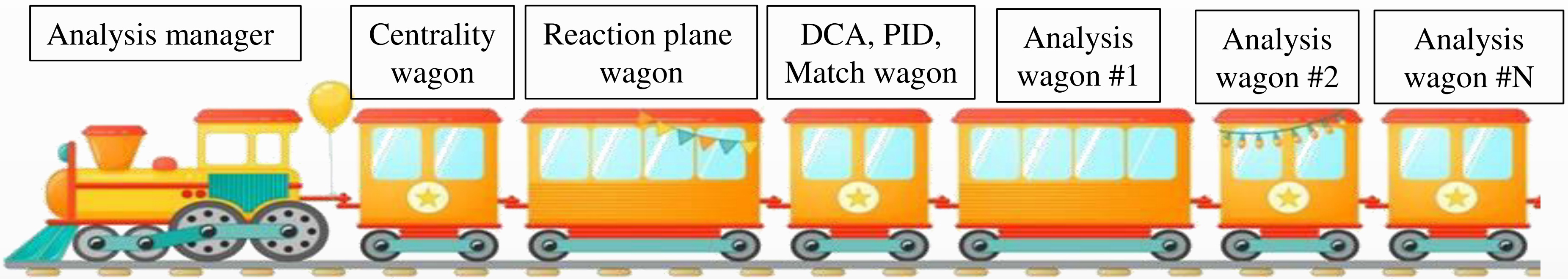

- First Analysis Train runs started in September, 2023 → regular runs on request ever since
- Many new services and improvements
- Train become a new standard for physics (feasibility) studies

Preparing for real data analysis, develop realistic analysis methods and techniques

Initial state

QGP as a relativistic fluid

Collective flow

Anisotropic flow at RHIC/LHC

- Initial eccentricity and its fluctuations drive momentum anisotropy v_n with specific viscous modulation

Spatial anisotropy of the nuclear overlap region

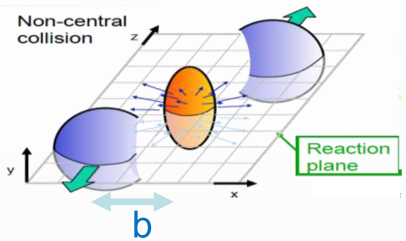

$$\epsilon_n = \sqrt{\frac{\langle r^n \cos n\phi\rangle + \langle r^n \sin n\phi\rangle}{\langle r^n\rangle}}$$

$\epsilon_n \propto v_n$

Azimuthal distribution of produced particles wrt to reaction plane (Ψ_n)

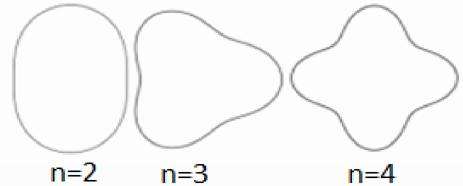

$$\frac{dN}{d\phi} \propto \left(1 + 2\sum_{n=1} v_n \cos\left[n\left(\phi - \Psi_n\right)\right]\right)$$

Anisotropic flow: $v_n = \langle \cos[n(\varphi - \Psi_n)]\rangle$

- Evidence for a dense perfect liquid found at RHIC/LHC (M. Roirdan et al., Scientific American, 2006)

Gale, Jeon et al., Phys. Rev. Lett. 110, 012302

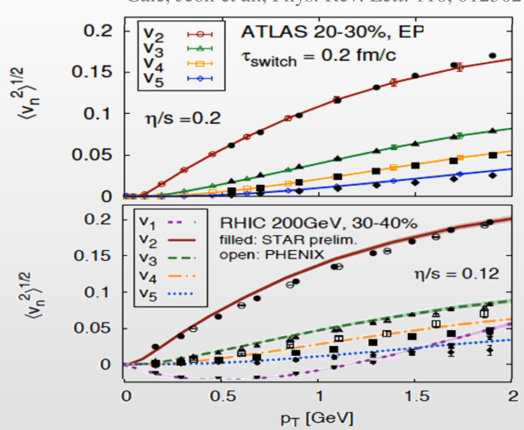

Phys.Rev.C 92 (2015) 3, 034913

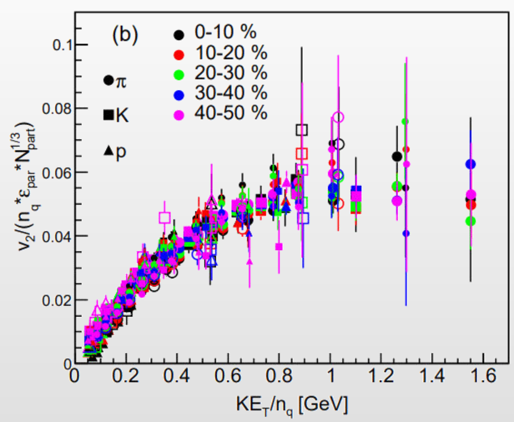

Phys. Rev. Lett. 122 (2019) 172301

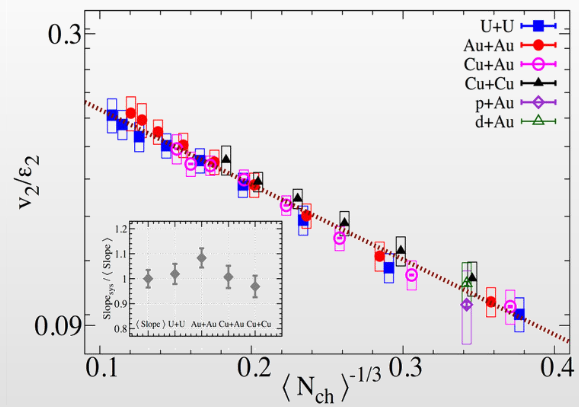

System size scan (p-A, A-A) is an important ingredient:

initial geometry → flow harmonics → $\frac{\eta}{s}(T,\mu), \frac{\zeta}{s}(T,\mu), c_s(T), \alpha_s(T), etc.$

See talk: Arkadiy Taranenko, System size scan at NICA energies

MPD performance for v_1, v_2 of V0 particles

❖ BiBi@9.2 GeV (PHSD, 15M), full event reconstruction

Differential flow can be defined using the following fit:

$$v_n^{SB}(m_{inv}) = v_n^S \frac{N^S(m_{inv})}{N^{SB}(m_{inv})} + v_n^B(m_{inv}) \frac{N^B(m_{inv})}{N^{SB}(m_{inv})}$$

- v_n^S - signal anisotropic flow (set as a parameter in the fit)
- $v_n^B(m_{inv})$ - background flow (set as polynomial function)

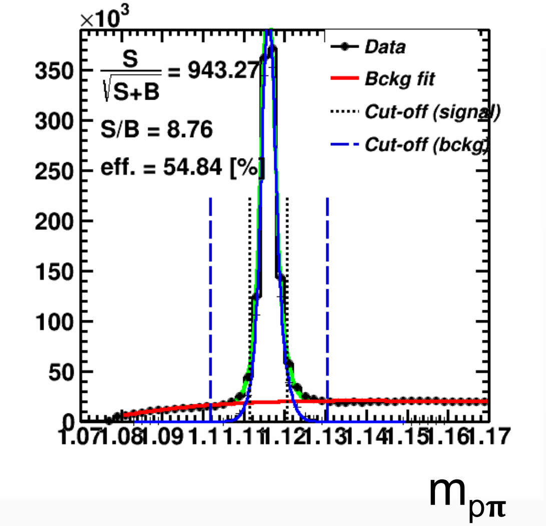

❖ Performance of v_1 and v_2 of Λ hyperons:

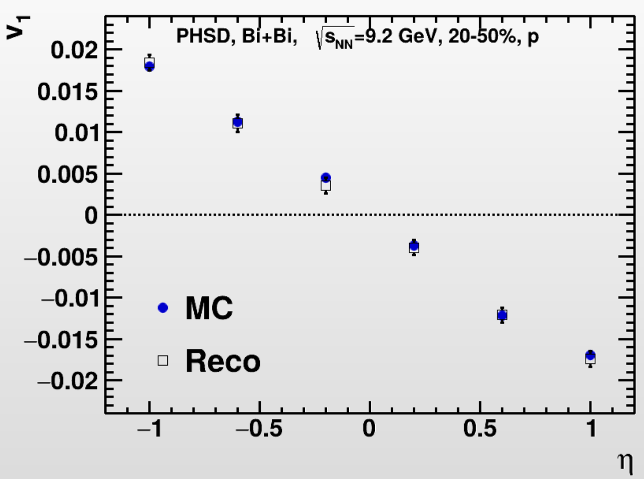

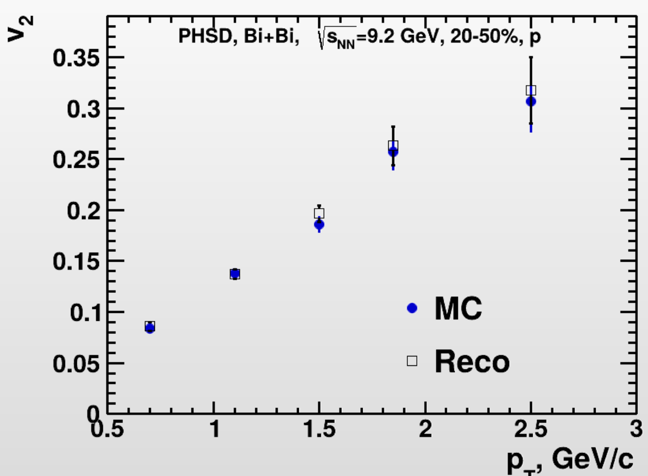

❖ Good performance for v_1, v_2 using invariant mass fit and event plane methods

❖ Similar measurements for Ks, other hyperons and short-lived resonances

MPD performance for v_1, v_2 of π/K/p

❖ BiBi@9.2 GeV (UrQMD, 50M), full event reconstruction

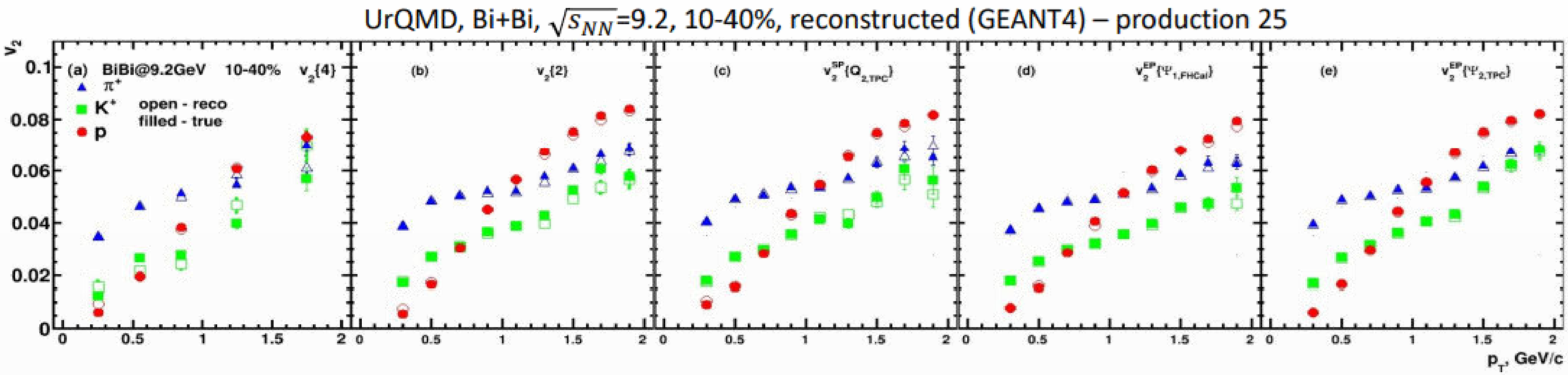

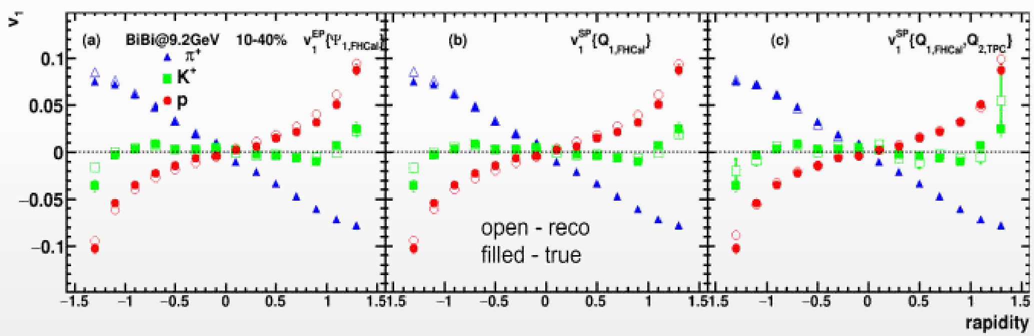

❖ Reconstructed and generated v_1 and v_2 for identified hadrons are in good agreement for all methods

MPD has capabilities to measure different flow harmonics for a wide variety of identified hadrons

System size scan for flow measurements is vital for understanding of the medium transport properties and onset of the phase transition

See talks:
Peter Parfenov: MPD performance in the fixed-target mode
Mikhail Mamaev: First flow results from BM@N experiment

Initial state

QGP as a relativistic fluid

Global polarization of particles

Non-central heavy-ion collisions

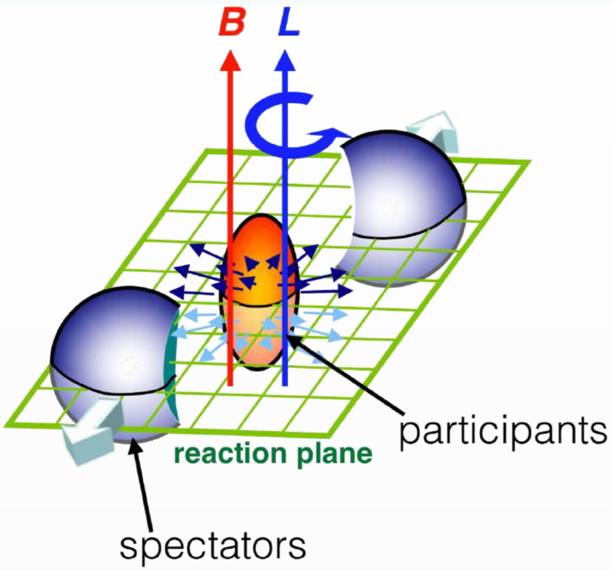

Large angular momentum due to medium rotations

Beccattini et al., PRC 77 (2008) 024906

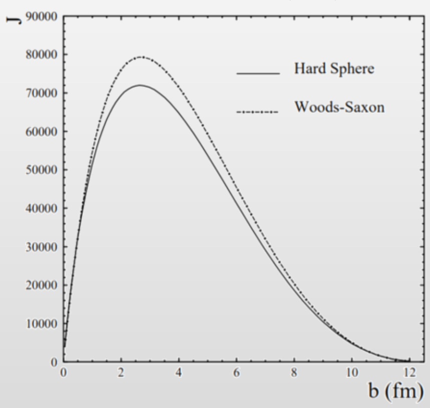

Strong magnetic field (~ 10^{13} T) formed for a short period of time

Kharzeev et al., NPA 803 (2008)

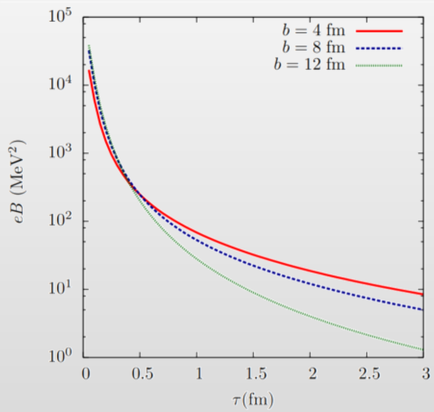

Focus is to see the effect of large angular momentum and magnetic field in heavy-ion collisions

Hyperon global polarization

❖ Global polarization of hyperons experimentally observed, decreases with $\sqrt{s_{NN}}$

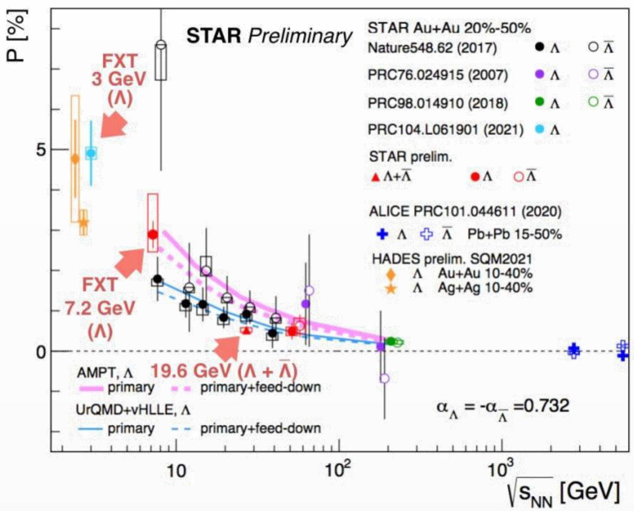

✓ reproduced by AMPT, 3FD, UrQMD+vHLLE

✓ hint for a Λ-$\bar{\Lambda}$ difference, magnetic field: ,

$$P_{\Lambda} \simeq \frac{1}{2}\frac{\omega}{T} + \frac{\mu_{\Lambda} B}{T} \qquad P_{\bar{\Lambda}} \simeq \frac{1}{2}\frac{\omega}{T} - \frac{\mu_{\Lambda} B}{T}$$

NICA: <u>extra points in the energy range 2-11 GeV</u>
centrality, p_T and rapidity dependence of polarization,
not only for Λ, but other (anti)hyperons (Λ, Σ, Ξ)

❖ MPD performance: BiBi@9.2 GeV (PHSD, 15 M events) → full reconstruction → Λ global polarization

Performance study of the hyperon global polarization measurements with MPD at NICA, Eur.Phys.J.A 60 (2024) 4, 85

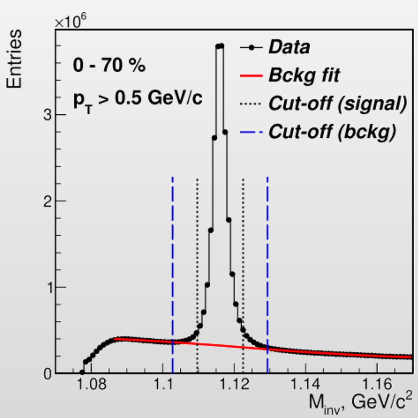

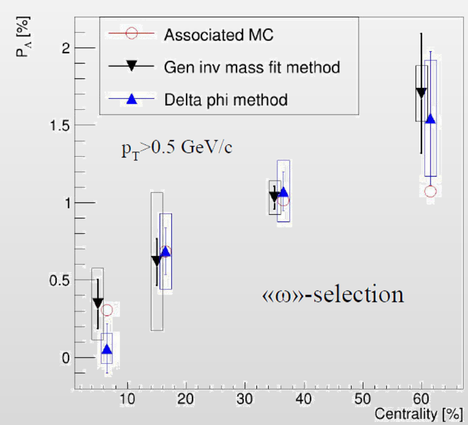

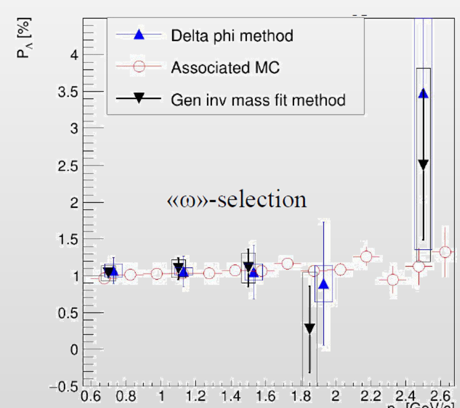

MPD: first global polarization measurements for $\Lambda/\bar{\Lambda}$ will be possible with ~ 10M data sampled events

Polarization of vector mesons: $K^*(892)$ and ϕ

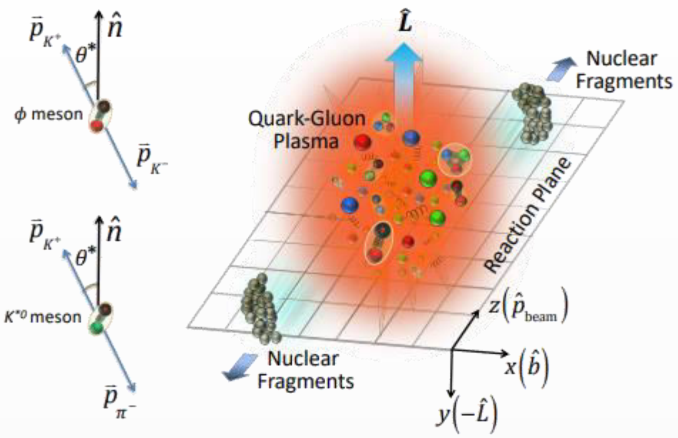

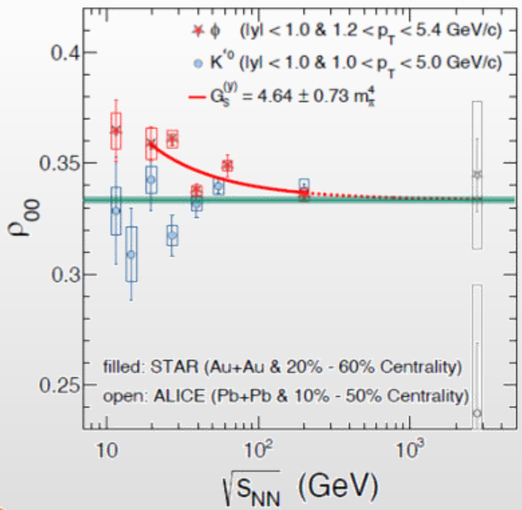

- Light quarks can be polarized by $|\bar{J}|$and $|\bar{B}|$
- If vector mesons are produced via recombination their spin may align
- Quantization axis:
  - ✓ normal to the production plane (momentum of the vector meson and the beam axis)
  - ✓ normal to the event plane (impact parameter and beam axis)
  - ✓ ρ_{00} (PP) - $\frac{1}{3}$ =[ρ_{00} (EP) - $\frac{1}{3}$] [$\frac{1+3v_2}{4}$]
- Measured as anisotropies:

$$\frac{dN}{dcos\theta} = N_0\left[1 - \rho_{0,0} + cos^2\theta\left(3\rho_{0,0} - 1\right)\right]$$

$\rho_{0,0}$ is a probability for vector meson to be in spin state = 0
→ $\rho_{0,0}$ = 1/3 corresponds to no spin alignment

- Measurements at RHIC/LHC challenge theoretical understanding → ρ_{00} can depend on multiple physics mechanisms (vorticity, magnetic field, hadronization scenarios, lifetimes and masses of the particles)

MPD: extend measurements in the NICA energy range, $\sqrt{s_{NN}}$ < 11 GeV

Initial state

QGP as a relativistic fluid

Hadronic resonances

Hadronic phase

- Short-lived resonances are sensitive to rescattering and regeneration in the hadronic phase

	ρ(770)	K*(892)	Σ(1385)	Λ(1520)	Ξ(1530)	ϕ(1020)
cτ (fm/c)	1.3	4.2	5.5	12.7	21.7	46.2
$\sigma_{rescatt}$	$\sigma_\pi\sigma_\pi$	$\sigma_\pi\sigma_K$	$\sigma_\pi\sigma_\Lambda$	$\sigma_K\sigma_p$	$\sigma_\pi\sigma_\Xi$	$\sigma_K\sigma_K$

- Properties of the hadronic phase are studied by measuring ratios of resonance yields to yields of long-lived particles with same/similar quark contents: ρ/π, K*/K, ϕ/K, Λ*/Λ, $\Sigma^{*\pm}/\Sigma$ and Ξ^{*0}/Ξ

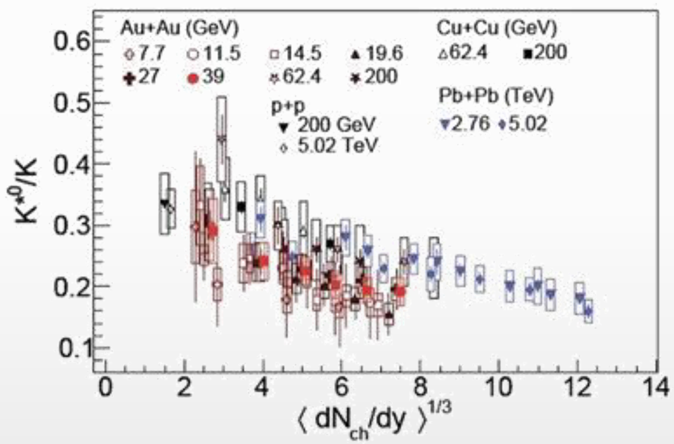

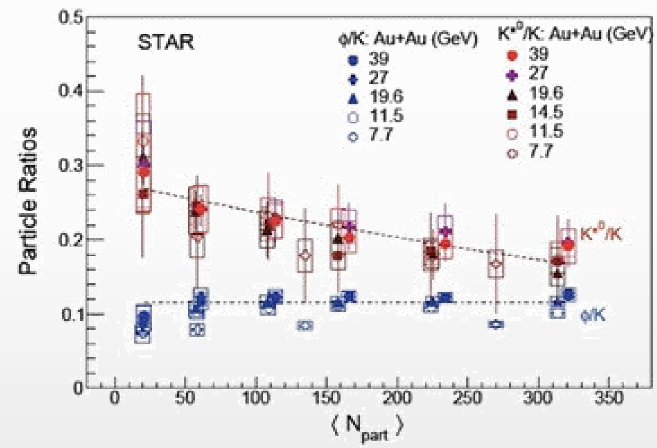

- Measurements in a wide energy range $\sqrt{s_{NN}}$= 7-5000 GeV support the existence of a hadronic phase that lives long enough (up to τ ~ 10 fm/*c*) to cause a significant reduction of the reconstructed yields of short-lived resonances
- All model predictions for early stages must be filtered through the hadronic phase

Precise measurements at NICA are needed to validate description of the hadronic phase in models

MPD performance for hadronic resonances

- BiBi@9.2 GeV (UrQMD, 50 M events), full event reconstruction
- Most realistic approach to data analysis, centrality dependence

ϕ(1020)

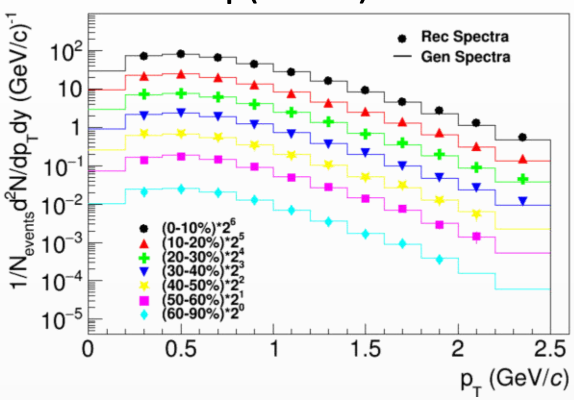

K*(892)⁰

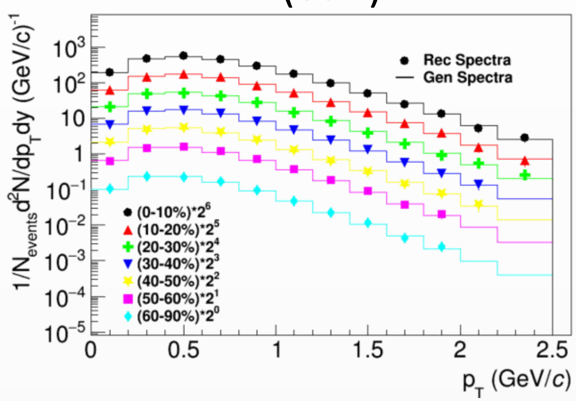

K*(892)±

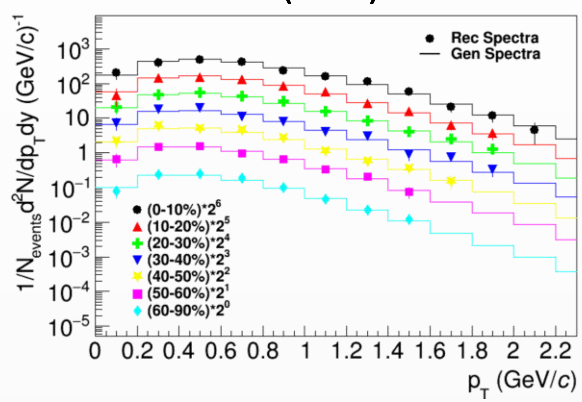

Λ(1520)

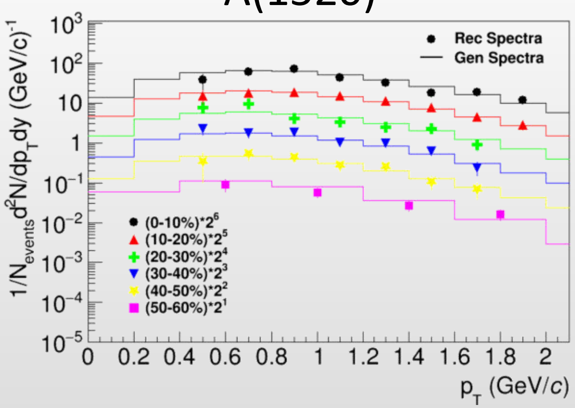

Σ(1385)±

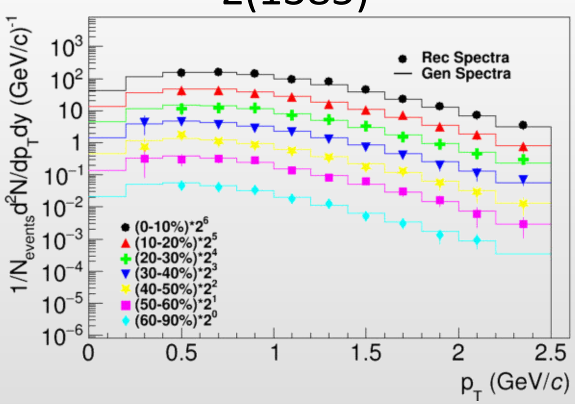

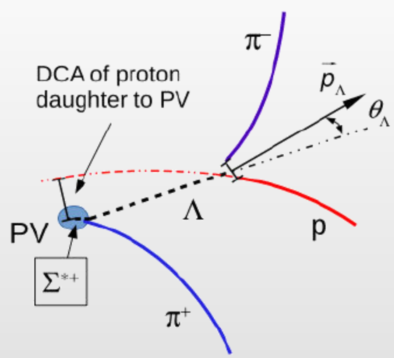

- Reconstructed spectra match truly generated ones within uncertainties
- Measurements are possible starting from ~ zero momentum → sample most of the yields

First centrality dependent studies with 50 M sampled A+A events

Initial state

QGP as a relativistic fluid

Strangeness production

Strange baryons

- Since the mid 80s, strangeness enhancement is considered as a signature of the QGP formation
- Experimentally observed in heavy-ion collisions at AGS, SPS, RHIC, and LHC energies.

NA57 and WA97 at SPS

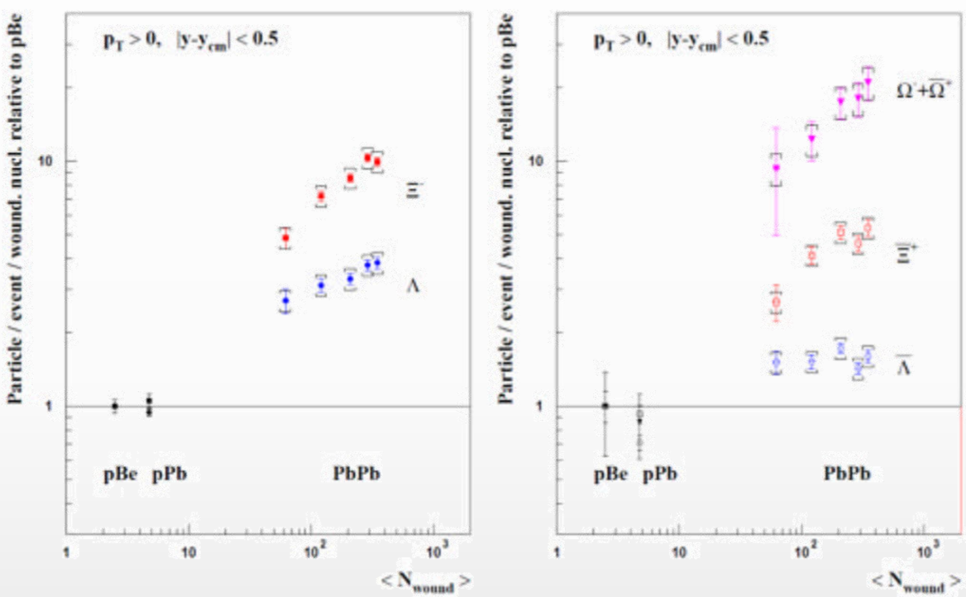

RHIC/LHC

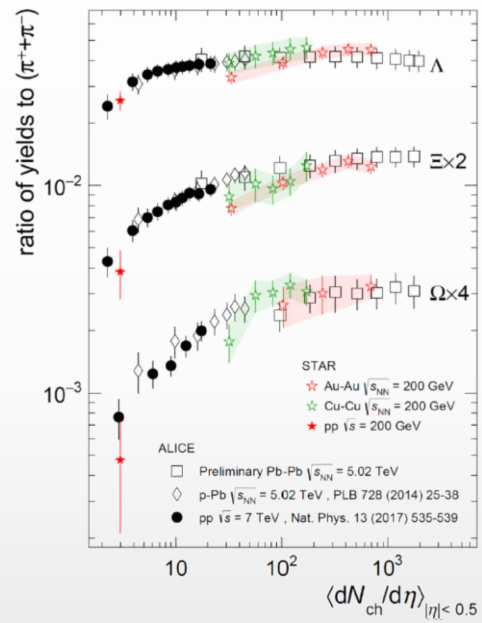

- No consensus on the dominant strangeness enhancement mechanisms:
  - ✓ strangeness enhancement in QGP contradicts with the observed collision energy dependence
  - ✓ strangeness suppression in pp within canonical suppression models reproduces most of results except for ϕ(1020)
- System size scan (pp, p-A, A+A) + differential measurements (vs. p_T, multiplicity, event shape, energy balance) of (multi)strange baryons and mesons is a key to understanding of strangeness production

System size scan in the NICA energy range is important

MPD performance for hyperons

- BiBi@9.2 GeV (UrQMD, 50M events), full event reconstruction

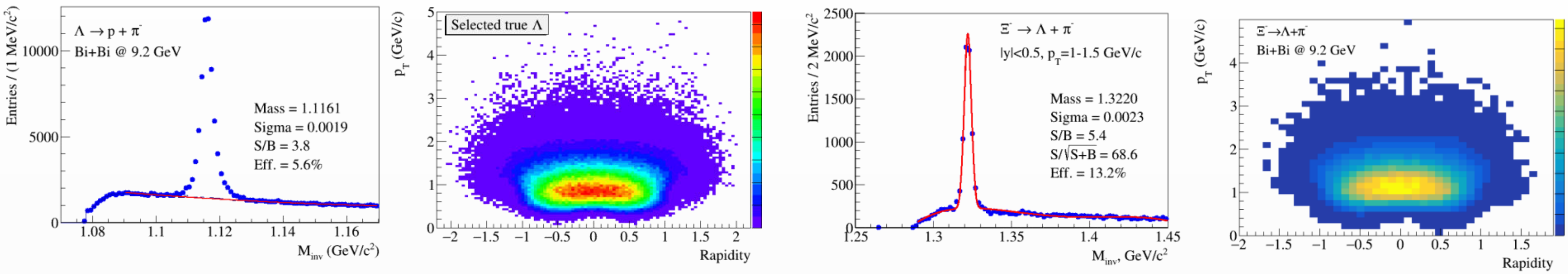

- different background estimates (fit function vs mixed-event), testing alternative Machine Learning techniques
- different PID selections for high-p_T daughter particles

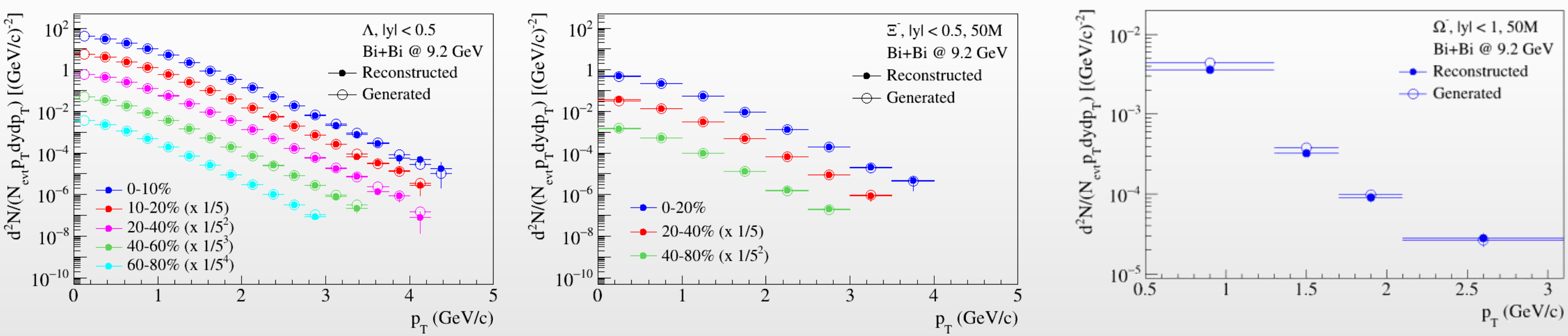

MPD has capabilities to measure production of strange kaons, (multi)strange baryons and resonances in pp, p-A and A-A collisions using h-ID in the TPC&TOF and different decay topology selections

See talks:
Alexander Zinchenko, Study of hyperon and hypernuclei production at NICA
Vadim Kolesnikov: Study of hadron and light nuclei production at NICA

Initial state

QGP as a relativistic fluid

Electromagnetic radiation

Direct photons and system temperature

- Direct photons are all photons except for those coming from hadron decays:
  - ✓ produced during all stages of the collision
  - ✓ QGP is transparent for photons → penetrating probe
- Low-E photons → effective temperature of the system:

$$E_\gamma \frac{d^3 N_\gamma}{d^3 p_\gamma} \propto e^{-E_\gamma / T_{\mathrm{eff}}}$$

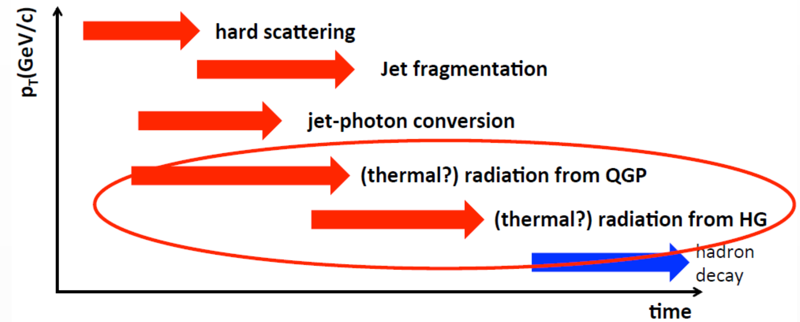

- Relativistic A+A collisions → the highest temperature created in laboratory ~ 10^{12} K

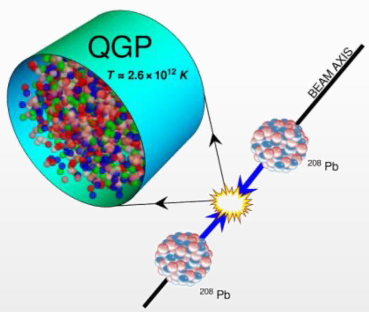

Temperature at the center of the Sun ~ 15 000 000 K

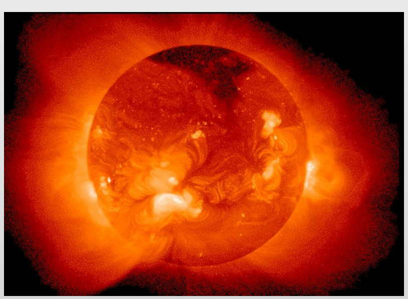

A medium of ~ 200 MeV is 100 000 times hotter !!!

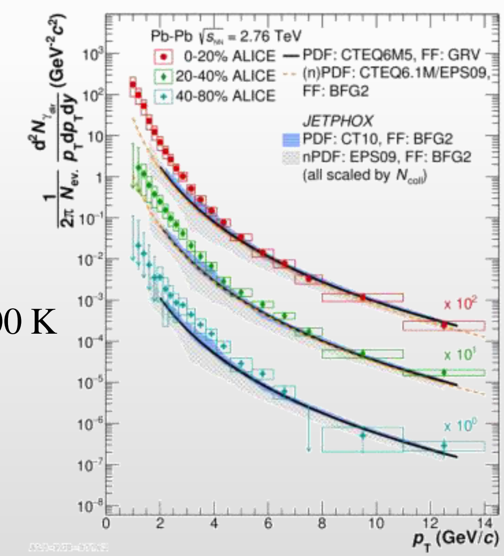

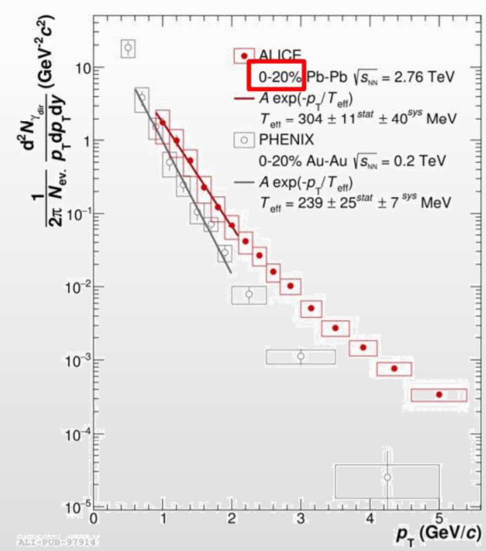

T_{eff} ~ 240 MeV at RHIC; T_{eff} ~ 300 MeV at the LHC

T_{eff} >> T_c ~ 160 MeV predicted by LQCD

Predictions for NICA

- Experimental measurements in A+A collisions are available from the LHC (2.76-5 TeV), RHIC (62-200 GeV) and WA98 (17.2 GeV)
- No measurements at NICA energies (direct photon yields and flow vs. p_T and centrality)

Estimation of the direct photon yields @NICA

model calculations

empirical scaling

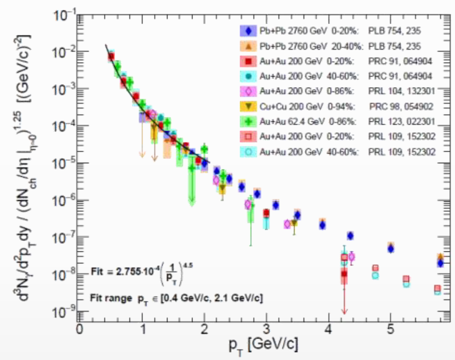

- ○ UrQMD v3.4 with hybrid model (3+1D hydro, bag model EoS, hadronic rescattering and resonances within UrQMD)
- ○ Each cell have Ti, Ei, µbi:
  - T is high – QGP phase (Peter Arnold, Guy D. Moore, Laurence G. Yaffe, JHEP 0112:009 2001)
  - T is low – HG phase (Simon Turbide, Ralf Rapp, Charles Gale, Phys.Rev.C69:014903,2004)
  - T is intermediate – mixed phase
- ○ Integrate over all cells and all time steps
- ○ Calculations reproduce hydro calculations for the SPS

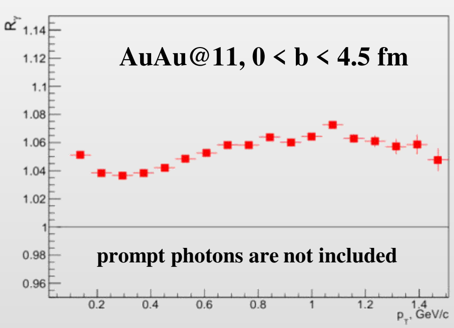

Phys.Part.Nucl. 52 (2021) 4, 681-685

$$R_\gamma = \frac{\gamma_{\rm inc}}{\gamma_{\rm decay}} = \frac{\gamma_{\rm inc}/\pi^0}{\gamma_{\rm decay}/\pi^0_{\rm param}}$$

$$\gamma_{\rm direct} = \left(1 - \frac{1}{R_\gamma}\right) \cdot \gamma_{\rm inc}$$

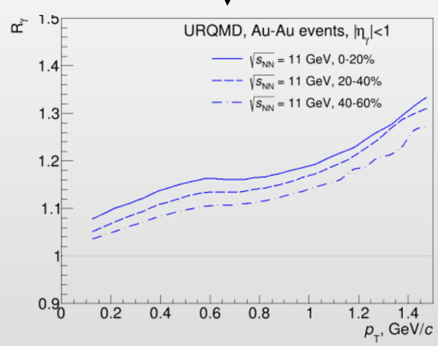

- Non-zero direct photon yields are predicted, Rγ ~ 1.05 – 1.15 → experimentally reachable!!!

Prospects for the MPD

- Photons can be measured in the ECAL or in the tracking system as e^+e^- conversion pairs (PCM)

beam pipe (0.3% X_0) + inner TPC vessels (2.4% X_0)

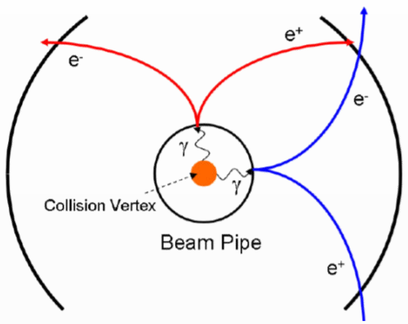

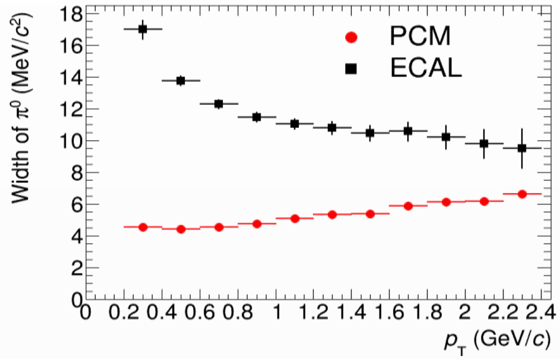

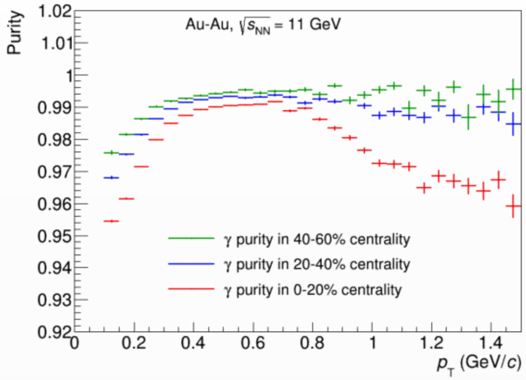

- ECAL high time-of-flight resolution is important for bckg. suppression at low-E (~ 100 ps) !!!
- Main sources of systematic uncertainties for direct photons:
  - ✓ detector material budget → conversion probability; p_T-shapes and reconstruction efficiencies of π^0 and η
  - ✓ with $R\gamma \sim 1.1$ and $\delta R\gamma/R\gamma \sim 3\%$ → uncertainty of $T_{eff} \sim 10\%$

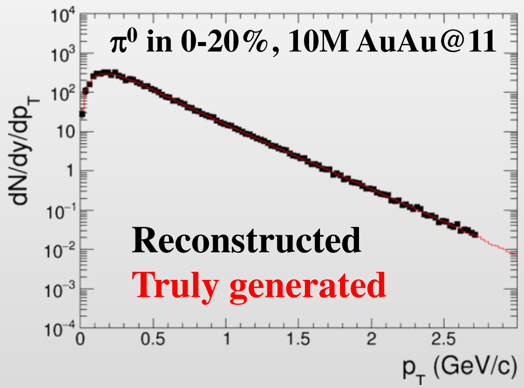

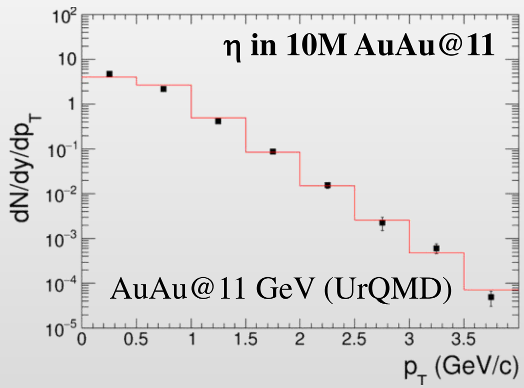

MPD can potentially provide measurements for direct photon production in the NICA energy range

Dielectron continuum and LVMs

- The QCD matter produced in A-A interactions is transparent for leptons, once produced they leave the interaction region largely unaffected + not sensitive to collective expansion
- Dielectron continuum carries a wealth of information about reaction dynamics and medium properties

PLB 753, 586 (2016)

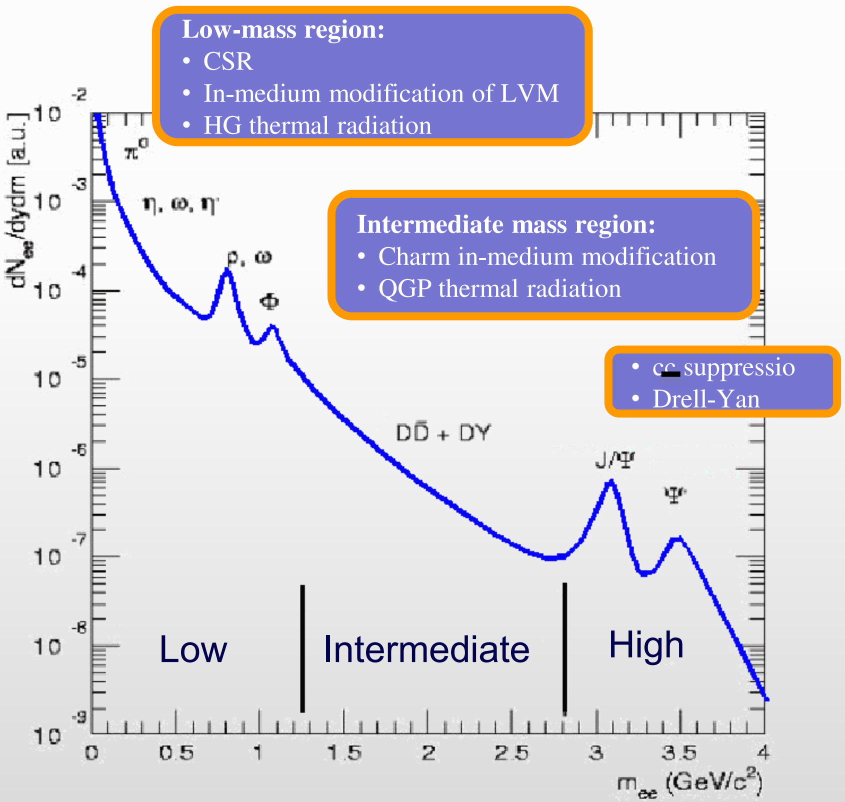

LMR as chronometer

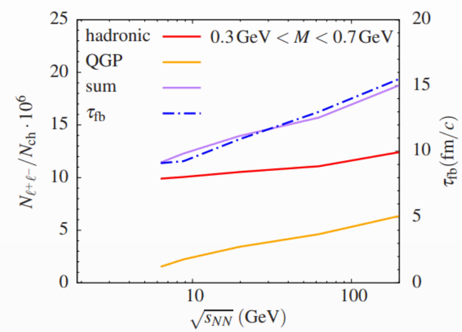

Integrated thermal excess radiation tracks the total fireball lifetime within ~ 10% → non-monotonous lifetime variations trace critical phenomena

IMR as thermometer

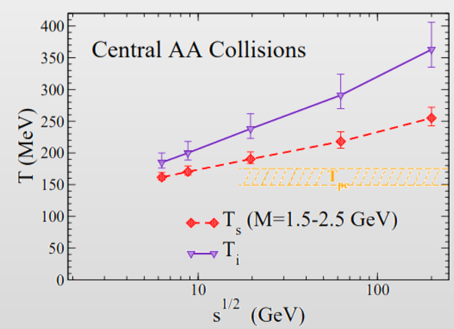

$dR_{ll}/dM \propto (MT)^{3/2} \exp(-M/T_s)$,

T_s smoothly evolves T = 160 MeV to 260 MeV

e-ID with MPD

❖ eID with TPC + TOF

n-sigma dE/dx parameterization

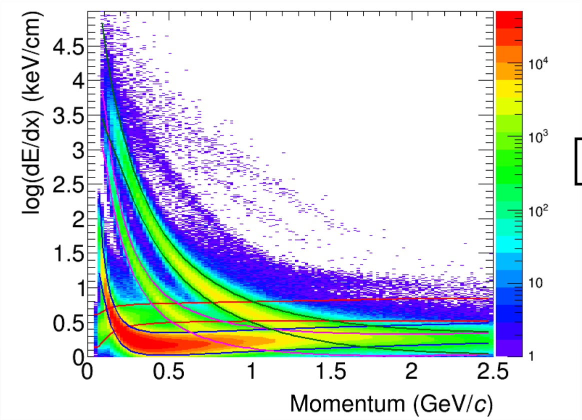

n-sigma β-TOF parameterization

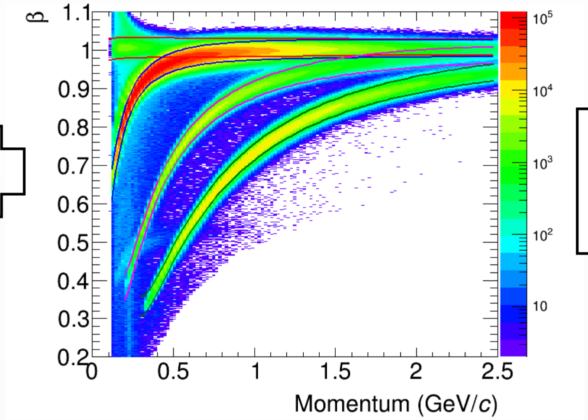

n-σ dE/dx distribution for tracks matched to TOF and identified as electrons

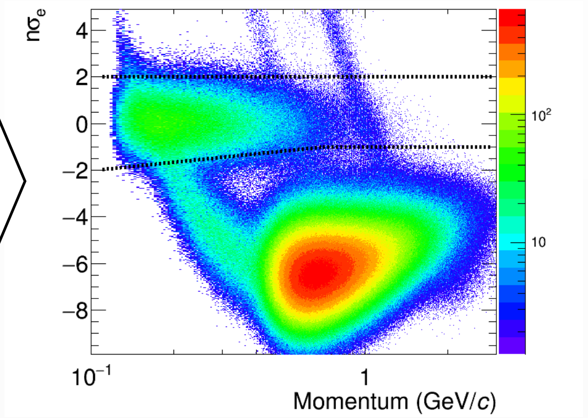

❖ eID with ECAL: steps in at higher energies where TPC/TOF become less effective

E/p for electron tracks

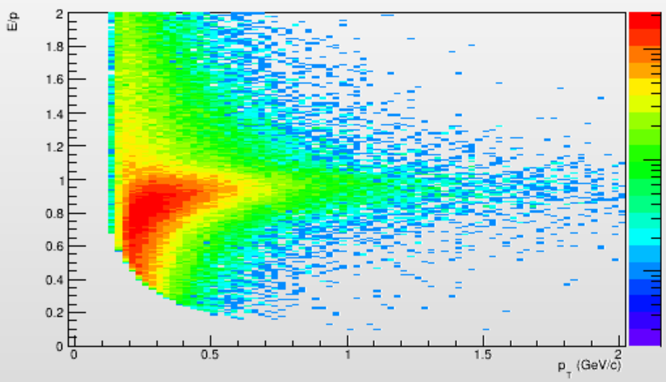

- ECAL e-ID for 2σ-matched tracks:
  - ✓ **TOF** < 2 ns (δ ~ 500 ps)
  - ✓ E/p ~ 1
- Turns on at p_T > 200 MeV/c

MPD performance for (di)electrons

- Electron reconstruction efficiency and purity, AuAu@11 (UrMQD v.3.4) events

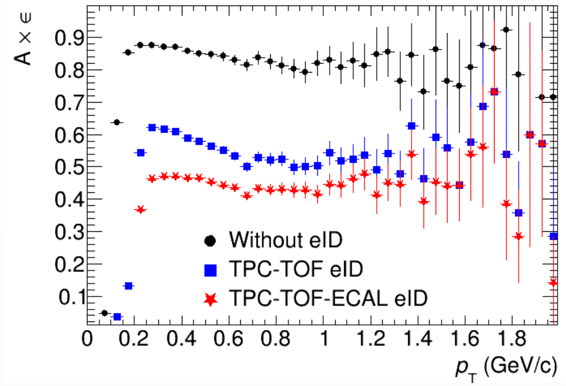

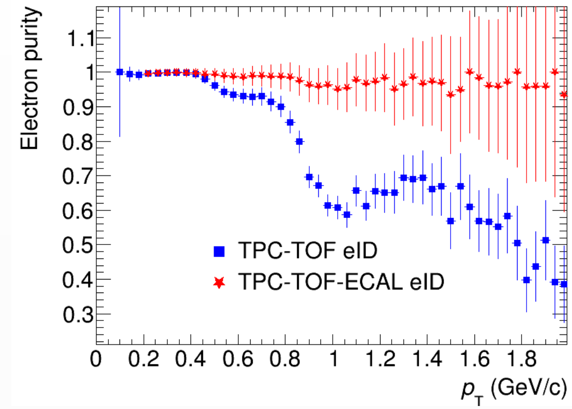

- Dielectron continuum

eID with TPC/TOF-eID

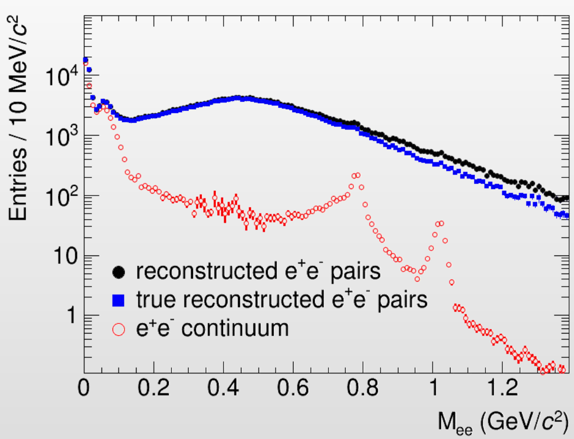

eID with TPC/TOF/EMC-eID

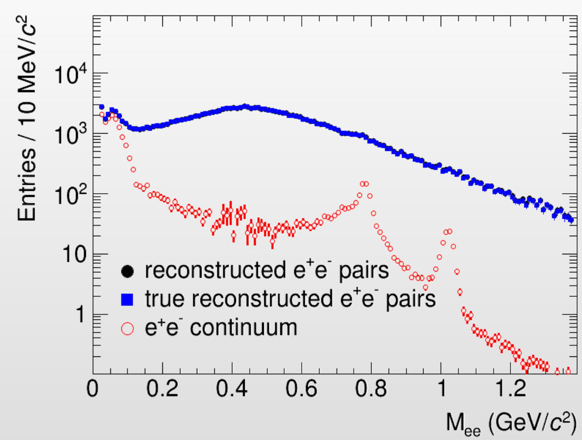

- MPD provides reconstruction of electrons with high purity
- S/B for dielectron measurements was achieved at 1/20 in the mass region 0.2-1.4 GeV/c^2

Summary

MPD Collaboration meeting in JINR (Dubna): April 23-25

- ❖ Heavy-ion collisions provide the means to study QCD phase diagram at extreme temperatures and (net)baryon densities. NICA energy range → moderate temperatures and maximum (net)baryon densities
- ❖ Preparation of the MPD detector and experimental program is ongoing, develop realistic analysis methods and techniques → MPD commissioning with beams in 2025
- ❖ MPD@NICA provides capabilities for important/unique contributions
- ❖ Many vacant (not so well covered) topics: fluctuations of conserved charges, HBT, dielectrons, etc.
- ❖ Next Collaboration meeting: 14-16 October → welcome !!!

BACKUP

NICA accelerator complex

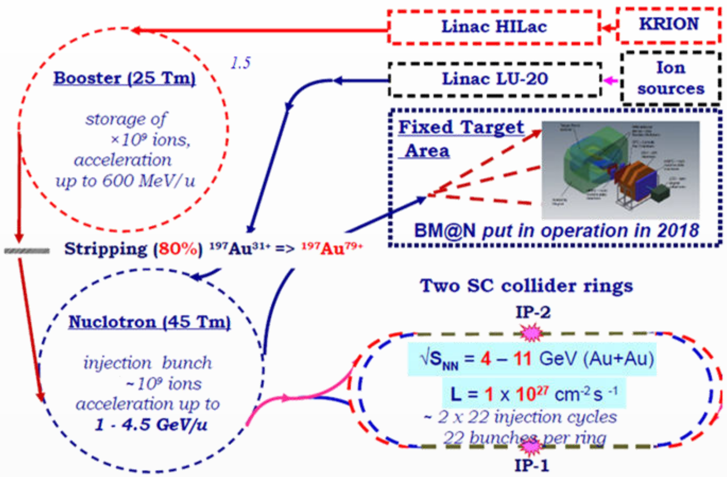

Booster

Nuclotron

❖ Stages of the accelerator complex commissioning:

- ✓ HILAC + transfer line to Booster → commissioned in 2018 with He^{1+}, Fe^{14+}, C^{4+}, Ar^{14+} and Xe^{28+}
- ✓ HILAC + Booster → first run in November-December, 2020 with He^{1+}
- ✓ HILAC + Booster + transfer line to Nuclotron → second run in October, 2021 with He^{1+} and Fe^{16+}
- ✓ HILAC + Booster + Nuclotron + transfer line to BM@N → third run in Jan. – Apr., 2022 with C^{6+}
- ✓ HILAC + Booster + Nuclotron + transfer line to BM@N -> fourth run in September, 2022 – February, 2023 with Ar and Xe beams → 500+ M events at BM@N

NICA collider

Nuclotron-NICA transfer line

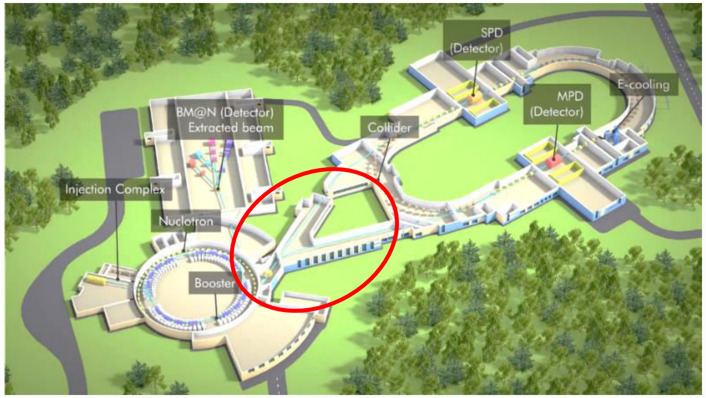

NICA collider

dipoles and quadrupoles have been installed in the tunnel

RF-1 и four RF-2 systems installed in the tunnel

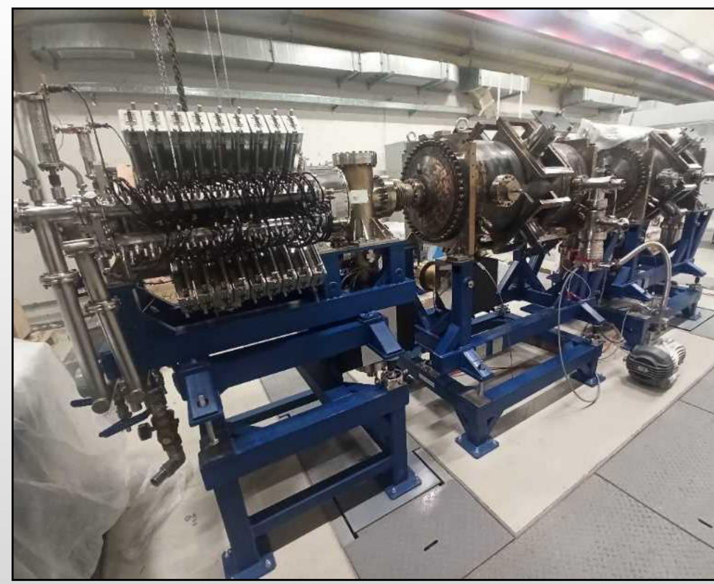

- ❖ Magnet and RF installation – nearly finalized
- ❖ Fast extraction system from the Nuclotron and Nuclotron-to-Collider transfer line – autumn of 2024
- ❖ First technological and cryogenic run of collider – end of 2024 - beginning of 2025
- ❖ First run with beams – second half of 2025

MPD @ NICA

❖ One of two experiments at NICA collider to study heavy-ion collisions at $\sqrt{s_{NN}}$= 4−11 GeV

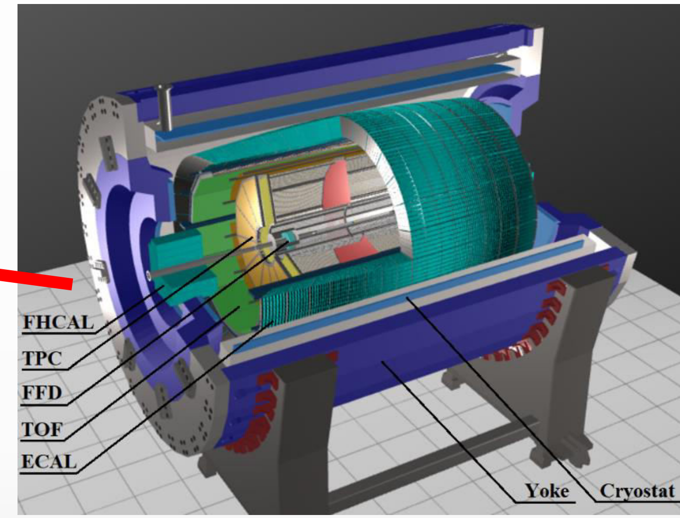

TPC: |Δφ| < 2π, |η| ≤ 1.6; **TOF, EMC**: |Δφ| < 2π, |η| ≤ 1.4; **FFD**: |Δφ| < 2π, 2.9 < |η| < 3.3; **FHCAL**: |Δφ| < 2π, 2 < |η| < 5

Au+Au @ 11 GeV (UrQMD + full chain reconstruction)

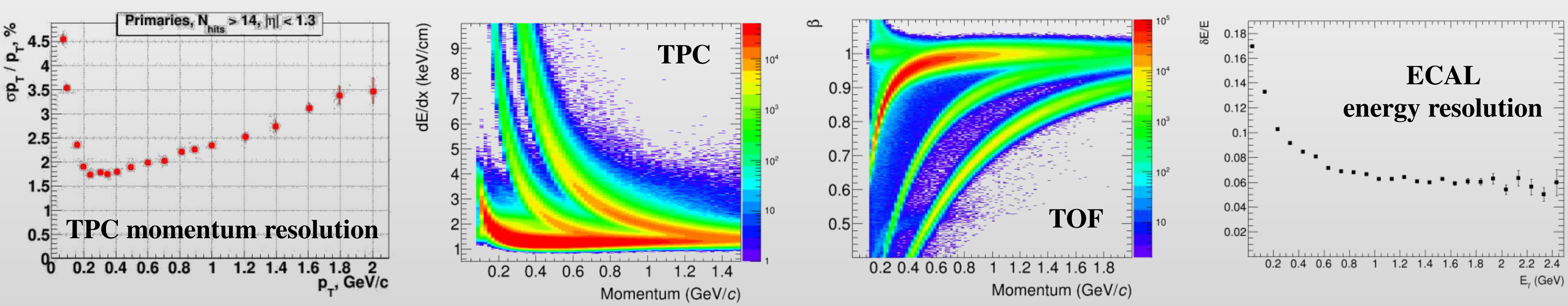

CLD: trigger simulation, BiBi@9.2 GeV

- Trigger system consists of FFD (2.7 < |η| < 4.1), FHCAL (2 < |η| < 5) and TOF (|η| < 1.5)
- MPD trigger system challenges at NICA energies:
  - ✓ low multiplicity of particles produced in heavy-ion collisions
  - ✓ particles are not ultra-relativistic (even the spectator protons)
  - ✓ wide z-vertex distribution, σ ~ 20 cm (σ ~ 50 cm at start-up)
- DCM-QGSM-SMM, BiBi@9.2: trigger efficiency is 87-98% for different trigger configuration

- FFD trigger definition:
  - ✓ at least one fired module per side
  - ✓ meaningful times, 0 < time $_{E,W}$ < 50 ns
  - ✓ reconstructed |z-vertex| < 140 cm
- FHCAL trigger definition:
  - ✓ at least one fired module per side
  - ✓ meaningful times, 0 < time $_{E,W}$ < 50 ns
  - ✓ reconstructed |z-vertex| < 150 cm
- TOF trigger definition:
  - ✓ at least one fired MRPC

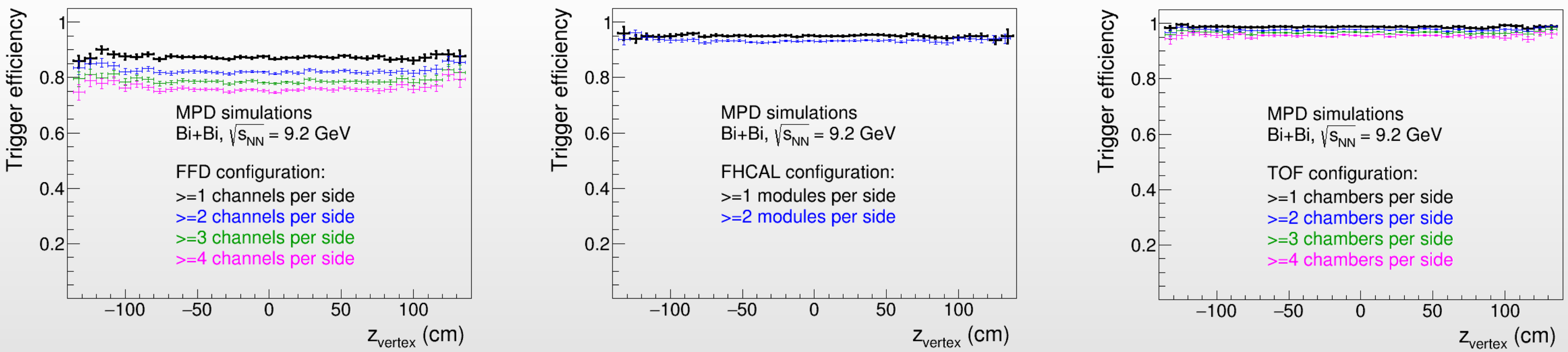

- Trigger system of the MPD based on FFD, FHCAL and TOF detectors provides high efficiency in HIC
- Simulation of the MPD trigger system is included in the Analysis Train
- Light collision systems: ~ 50% for C+C, vanishingly small for d+d

Need different solutions for triggering for light systems

FXT: trigger simulation, XeW@2.9 GeV

- Trigger system consists of FFD (2.7 < |η| < 4.1), FHCAL (2 < |η| < 5) and TOF (|η| < 1.5)
- MPD trigger system challenges at NICA energies:
  - ✓ no coincidence signals for East and West trigger detectors
  - ✓ particles are not ultra-relativistic (even the spectator protons)
- DCM-QGSM-SMM, XeW@2.9: trigger efficiency is 73-97% for different trigger configuration

• FFD trigger definition:
✓ at least one fired module (East)
✓ meaningful times, $0 < time_E < 50$ ns

• FHCAL trigger definition:
✓ at least one fired module (East)
✓ meaningful times, $0 < time_E < 50$ ns

• TOF trigger definition:
✓ at least one fired MRPC

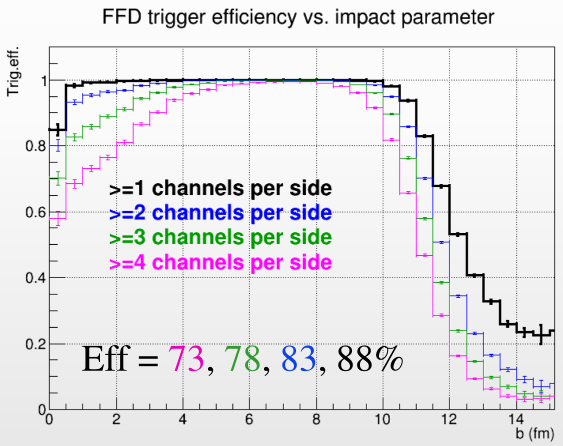

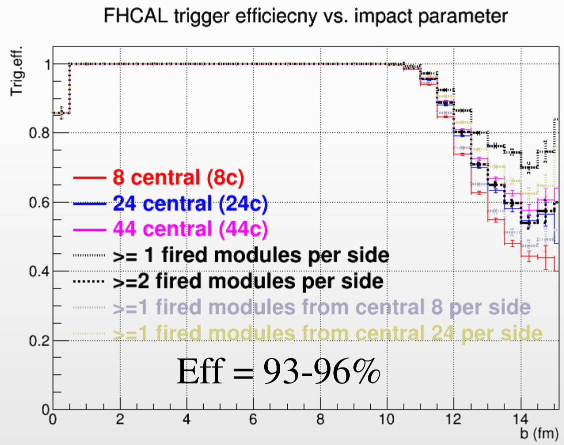

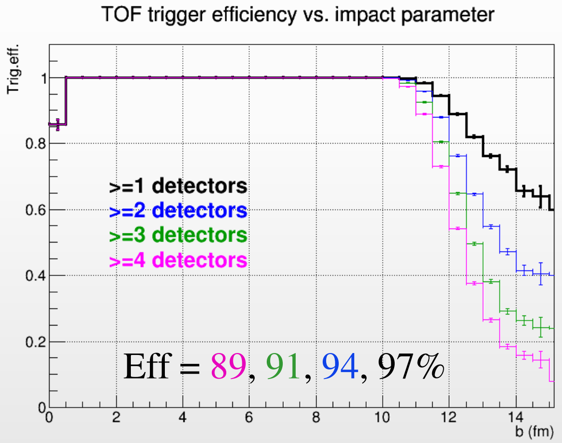

- Trigger system of the MPD based on FFD, FHCAL and TOF detectors remains efficient in FXT
- Need to better understand background (beam-gas, beam-pipe, etc.) and noise situation

Efficiency for π/K/p/Ks/Λ, z_{vertex} = - 85 cm

Basic track selections: $N_{hits} > 10$; DCA < 2 cm; primary particles ($R_{production} < 1$ cm)

❖ TPC-only tracks:

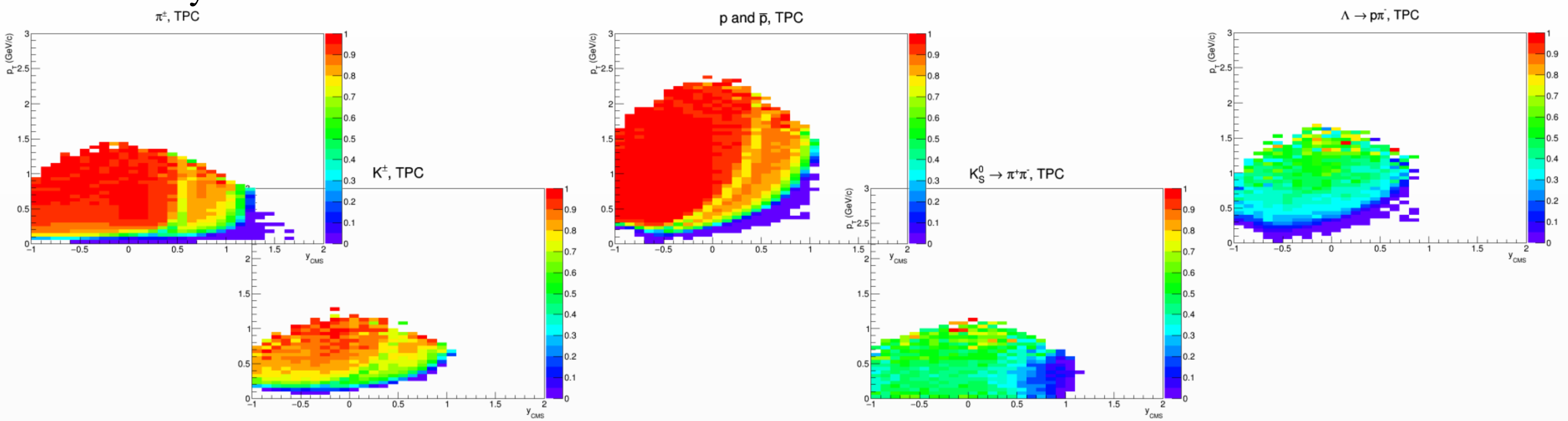

❖ TPC + TOF tracks:

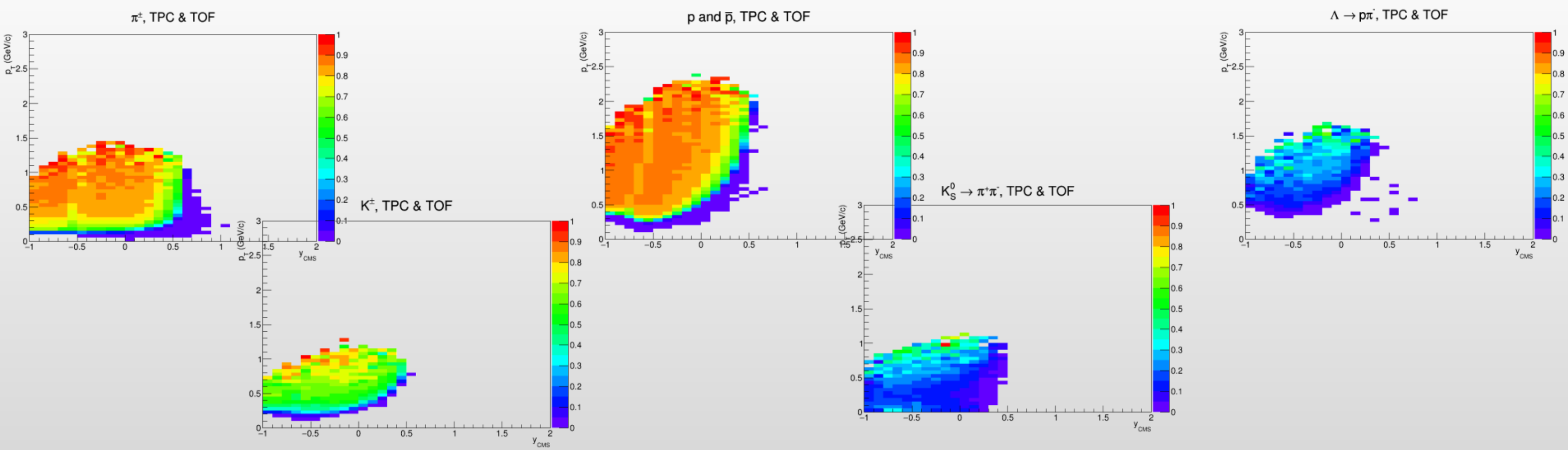

Reasonable coverage at mid-rapidity for light and heavy identified hadrons

MPD-FXT, v_1 & v_2 for protons/pions

- BiBi @ 2.5, 3.0 and 3.5 GeV (UrQMD mean-field, fixed-target mode)
- Realistic PID (TPC+TOF); efficiency corrections; centrality by TPC multiplicity

v_1 vs. rapidity

v_2 vs. p_T

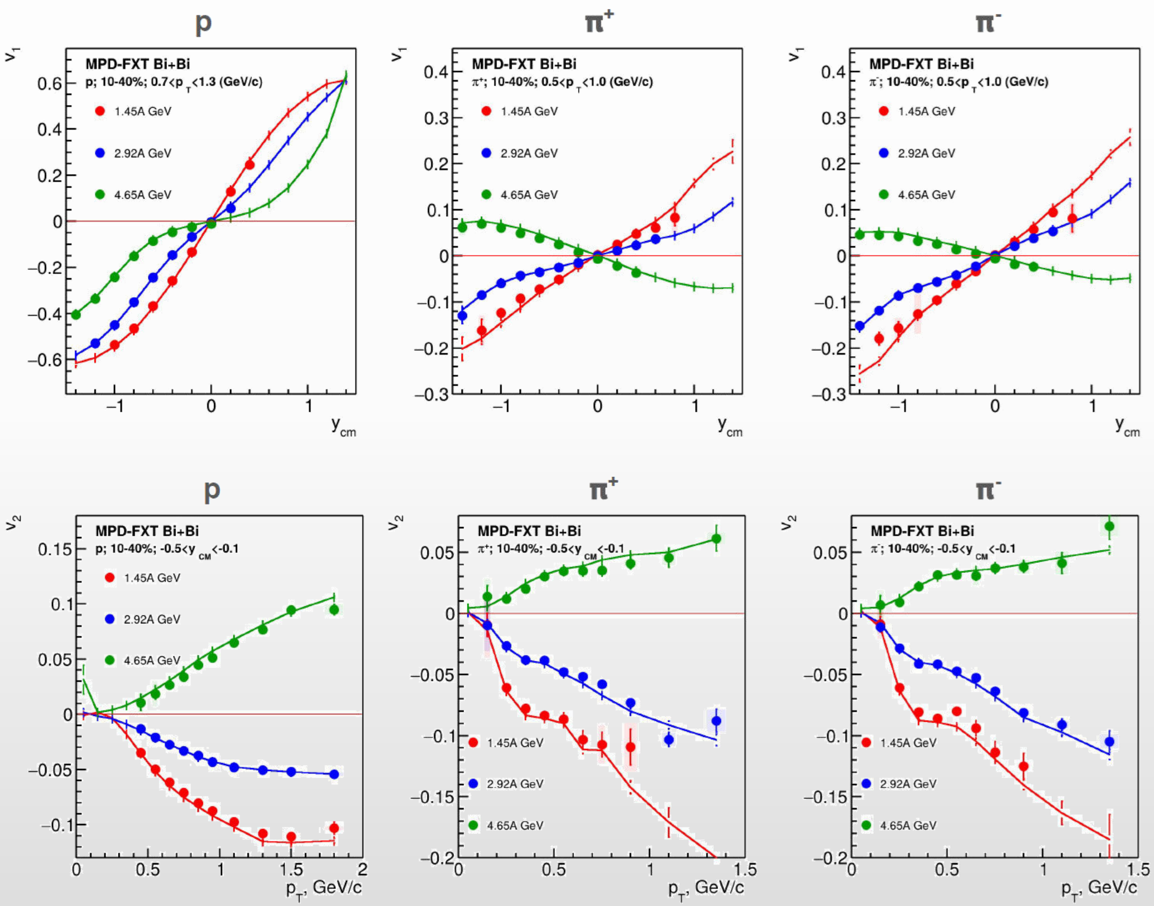

MPD vs. BM@N

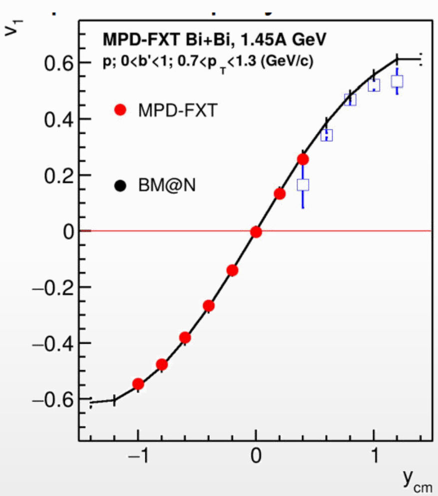

- Reconstructed v_1 & v_2 are quantitatively consistent with truly generated signals

MPD and BM@N complete each other with modest overlap

MPD performance for hypenuclei

❖ Mass production 29 (PHQMD, BiBi@9.2 GeV, 40M events)

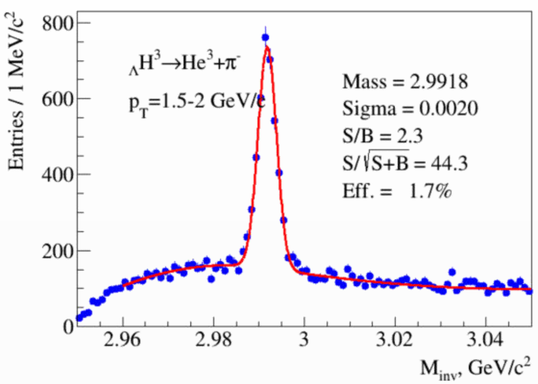

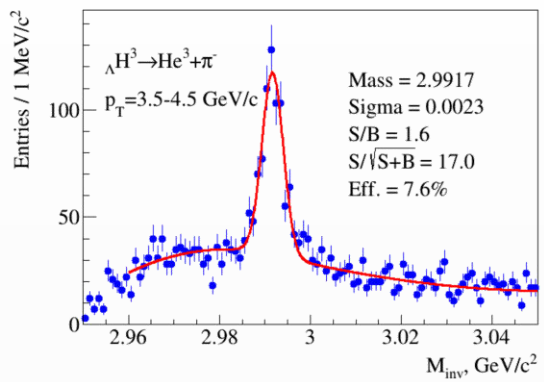

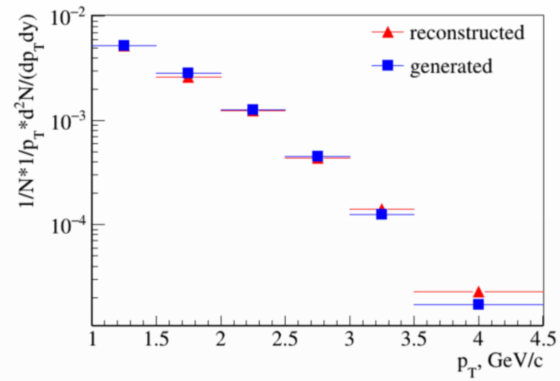

2- and 3-prong decay modes were studied separately to estimate systematics

$$N(\tau) = N(0)\exp\left(-\frac{\tau}{\tau_0}\right) = N(0)\exp\left(-\frac{ML}{cp\tau_0}\right),$$

Decay channel	Branching ratio	Decay channel	Branching ratio
$\pi^- + {}^3He$	24.7%	$\pi^- + p + p + n$	1.5%
$\pi^0 + {}^3H$	12.4%	$\pi^0 + n + n + p$	0.8%
$\pi^- + p + d$	36.7%	$d + n$	0.2%
$\pi^0 + n + d$	18.4%	$p + n + n$	1.5%

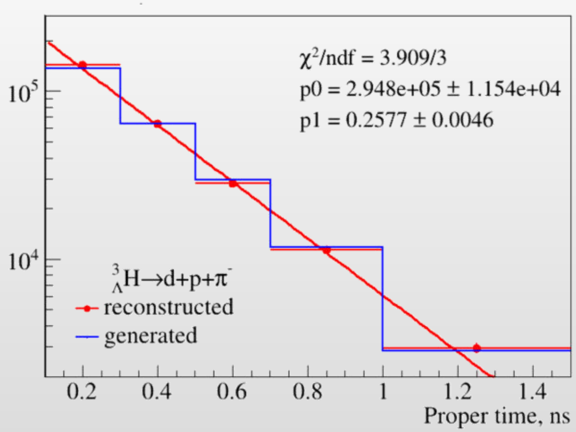

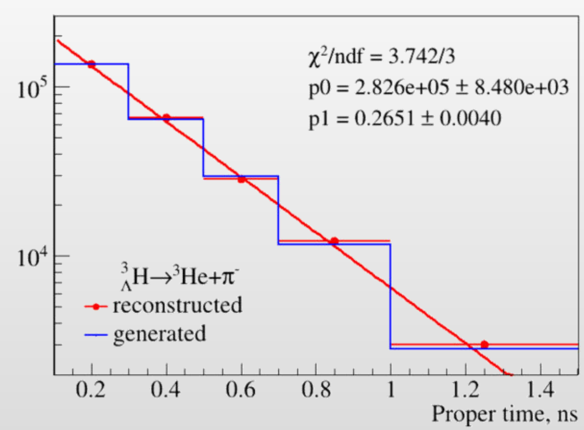

$_\Lambda H^3$ reconstruction with ~ 50M samples events

$_\Lambda H^4$, $_\Lambda He^4$ reconstruction with ~ 150M samples events

Direct photons puzzle(s)

❖ Simultaneous description of direct photon yields and elliptic flow (v_2) is problematic:

- ✓ direct photon flow is similar to flow of decay photons, underestimated by hydro → favors late emission
- ✓ large yields of low-E direct photon yields require early emission in to be described by hydro models

PRC 79 (2009) 021901

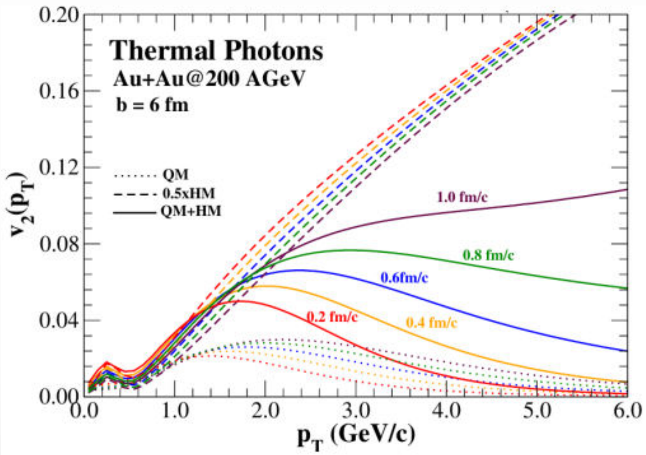

Phys.Lett.B 789 (2019) 308-322

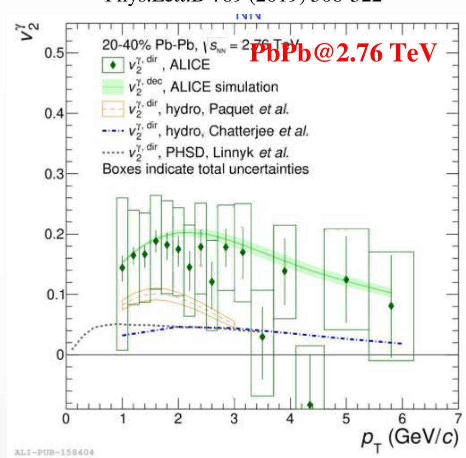

Phys.Rev. C94 (2016) no.6, 064901

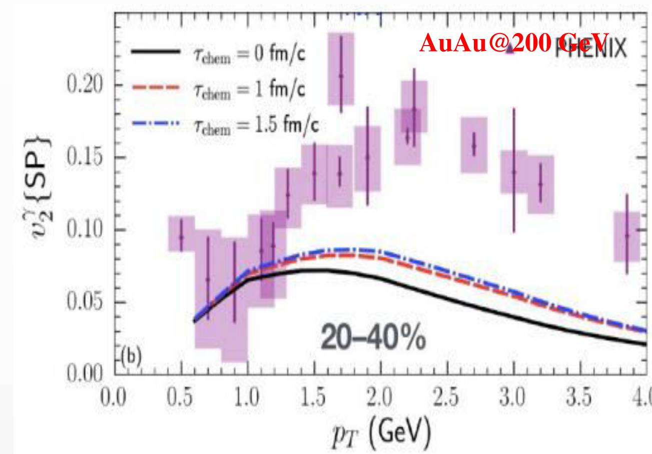

❖ Controversial results reported for different systems by different experiments

Quark Matter 2019, arxiv 2002.05191

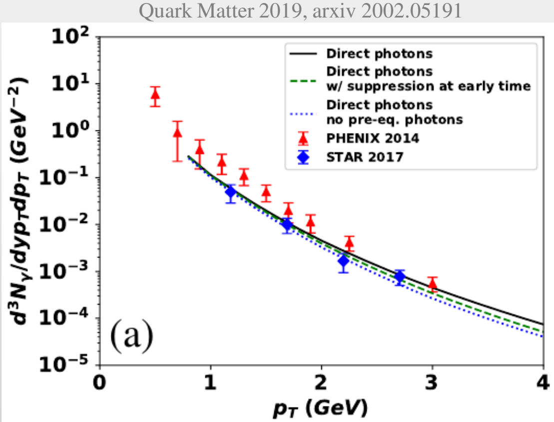

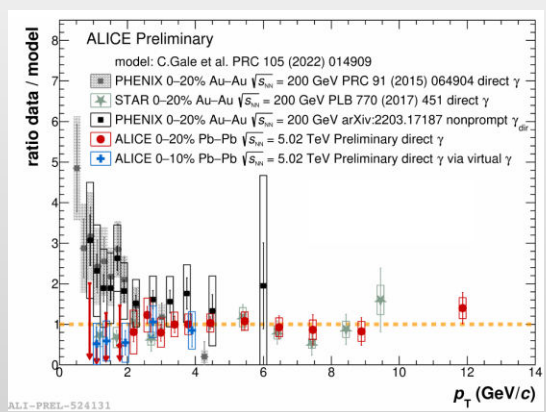

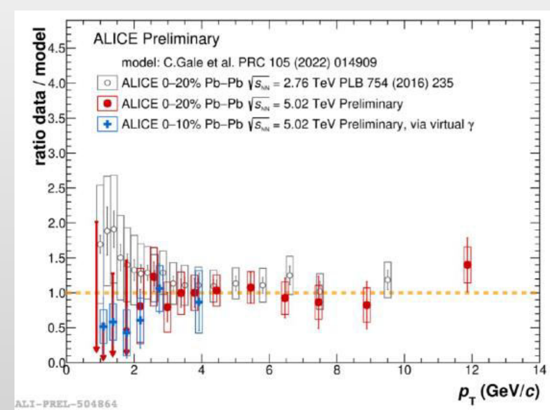

RHIC BES program

- Data taking by STAR at RHIC: 3 < $\sqrt{s_{NN}}$ < 200 GeV (750 < μ_B < 25 MeV)

Au+Au Collisions at RHIC

Collider Runs						Fixed-Target Runs					
	$\sqrt{s_{NN}}$ (GeV)	#Events	μ_B	y_{beam}	run		$\sqrt{s_{NN}}$ (GeV)	#Events	μ_B	y_{beam}	run
1	**200**	380 M	**25** MeV	5.3	Run-10, 19	1	13.7 (100)	50 M	280 MeV	-2.69	Run-21
2	62.4	46 M	75 MeV		Run-10	2	**11.5 (70)**	50 M	320 MeV	-2.51	Run-21
3	54.4	1200 M	85 MeV		Run-17	3	**9.2 (44.5)**	50 M	370 MeV	-2.28	Run-21
4	39	86 M	112 MeV		Run-10	4	**7.7 (31.2)**	260 M	420 MeV	-2.1	Run-18, 19, 20
5	27	585 M	156 MeV	3.36	Run-11, 18	5	7.2 (26.5)	470 M	440 MeV	-2.02	Run-18, 20
6	19.6	595 M	206 MeV	3.1	Run-11, 19	6	6.2 (19.5)	120 M	490 MeV	1.87	Run-20
7	17.3	256 M	230 MeV		Run-21	7	5.2 (13.5)	100 M	540 MeV	-1.68	Run-20
8	14.6	340 M	262 MeV		Run-14, 19	8	4.5 (9.8)	110 M	590 MeV	-1.52	Run-20
9	**11.5**	157 M	316 MeV		Run-10, 20	9	3.9 (7.3)	120 M	633 MeV	-1.37	Run-20
10	**9.2**	160 M	372 MeV		Run-10, 20	10	3.5 (5.75)	120 M	670 MeV	-1.2	Run-20
11	**7.7**	104 M	420 MeV		Run-21	11	3.2 (4.59)	200 M	699 MeV	-1.13	Run-19
						12	**3.0** (3.85)	2000 M	**750** MeV	-1.05	Run-18, 21

- A very impressive and successful program with many collected datasets, already available and expected results
- Limitations:
  - ✓ Au+Au collisions only
  - ✓ Among the fixed-target runs, only the 3 GeV data have full mid-rapidity coverage for protons (|y| < 0.5), which is crucial for physics observables

Au+Au @ 3.9 GeV

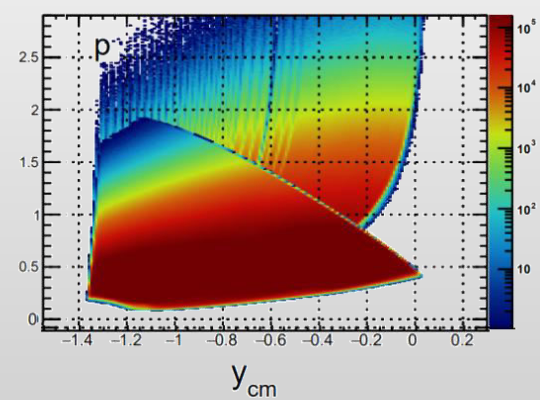

Polarization of Ξ and Ω

	Mass (GeV/c²)	cτ (cm)	decay mode	decay parameter	magnetic moment (μ_N)	spin
Λ (uds)	1.115683	7.89	Λ->πp (63.9%)	0.732±0.014	−0.613	1/2
Ξ⁻ (dss)	1.32171	4.91	Ξ⁻->Λπ⁻ (99.887%)	−0.401±0.010	−0.6507	1/2
Ω⁻ (sss)	1.67245	2.46	Ω⁻->ΛK⁻ (67.8%)	0.0157±0.002	-2.02	3/2

- Λ, Ξ and Ω have different spins and magnetic moments, different number of s-quarks, less feedback for heavier hyperons
- Direct measurements are difficult due to small values of α
- Measured based on polarization of daughter Λ

Phys. Rev. Lett. 126, 162301 (2021)

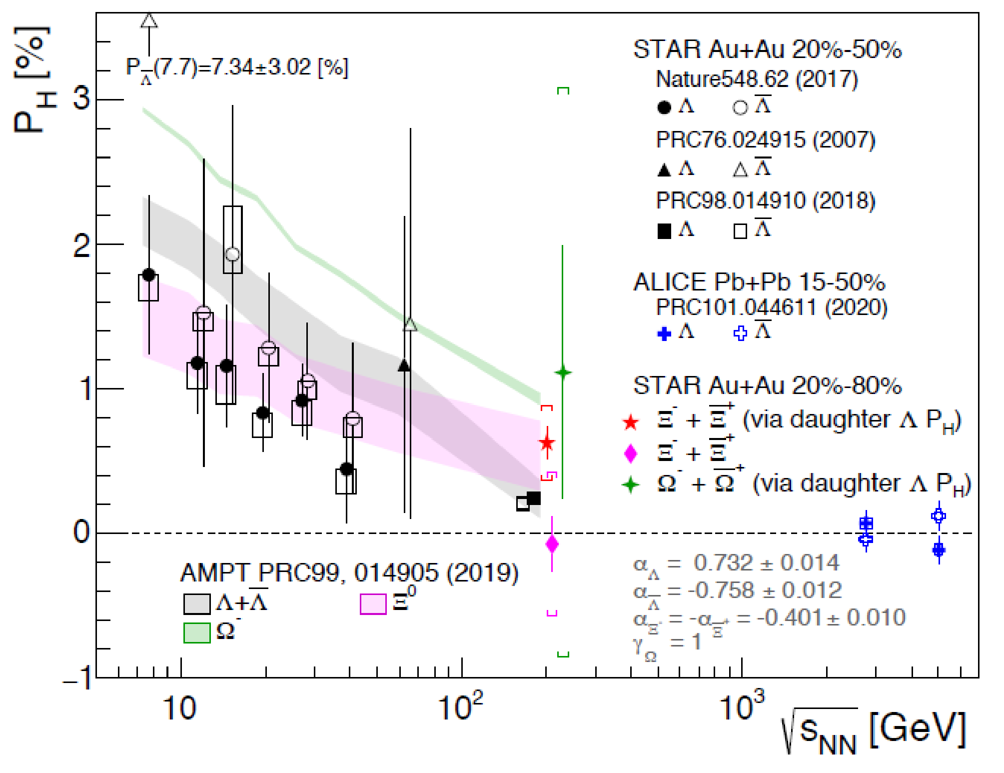

- AMPT is consistent with measurements
- Polarization of Ξ is larger compared with Λ:

$$\langle P_{\Lambda+\bar{\Lambda}}\rangle(\%) = 0.24 \pm 0.03 \pm 0.03$$

$$\langle P_{\Xi}\rangle = 0.47 \pm 0.10\ (\text{stat.}) \pm 0.23\ (\text{syst.})\ \%$$

- Λ results are not feed-back corrected (~ 15%)
- The AMPT is consistent with measurements
- Polarization of Ξ is larger compared with Λ
- Earlier freeze-out of multi-strange baryons is consistent with larger value of P_H for Ξ
- Large uncertainties for Ω, can expect larger signal, $P = \frac{\langle \bar{s} \rangle}{s} \sim \frac{s+1}{3}\frac{\bar{\omega}}{T}$ PRC95.054902 (2017)

Feed-down effect

- ~60% of measured Λ are feed-down from $\Sigma^* \to \Lambda \pi$, $\Sigma^0 \to \Lambda \gamma$, $\Xi \to \Lambda \pi$
- Polarization of parent particle R is transferred to its daughter Λ
  (Polarization transfer could be negative!)

$C_{\Lambda R}$: coefficient of spin transfer from parent R to Λ
S_R : parent particle's spin
$f_{\Lambda R}$: fraction of Λ originating from parent R
μ_R : magnetic moment of particle R

$$\mathbf{S}^*_\Lambda = C\mathbf{S}^*_R \qquad \langle S_y \rangle \propto \frac{S(S+1)}{3}(\omega + \frac{\mu}{S}B)$$

$$\begin{pmatrix} \varpi_c \\ B_c/T \end{pmatrix} = \begin{bmatrix} \frac{2}{3}\sum_R \left(f_{\Lambda R} C_{\Lambda R} - \frac{1}{3} f_{\Sigma^0 R} C_{\Sigma^0 R}\right) S_R(S_R+1) & \frac{2}{3}\sum_R \left(f_{\Lambda R} C_{\Lambda R} - \frac{1}{3} f_{\Sigma^0 R} C_{\Sigma^0 R}\right) (S_R+1)\mu_R \\ \frac{2}{3}\sum_{\overline{R}} \left(f_{\overline{\Lambda R}} C_{\overline{\Lambda R}} - \frac{1}{3} f_{\overline{\Sigma^0} \overline{R}} C_{\overline{\Sigma^0} \overline{R}}\right) S_{\overline{R}}(S_{\overline{R}}+1) & \frac{2}{3}\sum_{\overline{R}} \left(f_{\overline{\Lambda R}} C_{\overline{\Lambda R}} - \frac{1}{3} f_{\overline{\Sigma^0} \overline{R}} C_{\overline{\Sigma^0} \overline{R}}\right) (S_{\overline{R}}+1)\mu_{\overline{R}} \end{bmatrix}^{-1} \begin{pmatrix} P^{\rm meas}_\Lambda \\ P^{\rm meas}_{\overline{\Lambda}} \end{pmatrix}$$

Becattini, Karpenko, Lisa, Upsal, and Voloshin, PRC95.054902 (2017)

Decay	C
Parity conserving: $1/2^+ \to 1/2^+\ 0^-$	$-1/3$
Parity conserving: $1/2^- \to 1/2^+\ 0^-$	1
Parity conserving: $3/2^+ \to 1/2^+\ 0^-$	1/3
Parity-conserving: $3/2^- \to 1/2^+\ 0^-$	$-1/5$
$\Xi^0 \to \Lambda + \pi^0$	+0.900
$\Xi^- \to \Lambda + \pi^-$	+0.927
$\Sigma^0 \to \Lambda + \gamma$	$-1/3$

Primary Λ polarization will be diluted by 15%-20% (model-dependent)
This also suggests that **the polarization of daughter particles can be used to measure their parent polarization!** e.g. Ξ, Ω

Ξ and Ω polarization measurements

$$\frac{dN}{d\Omega^*} = \frac{1}{4\pi}\left(1 + \alpha_H \mathbf{P}_H^* \cdot \hat{\boldsymbol{p}}_B^*\right)$$

Getting difficult due to smaller decay parameter for Ξ and Ω…

$$\alpha_\Lambda = 0.732,\ \alpha_{\Xi^-} = -0.401,\ \alpha_{\Omega^-} = 0.0157$$

spin 1/2

Polarization of daughter Λ in a weak decay of Ξ:
(based on Lee-Yang formula)

T.D. Lee and C.N. Yang, Phys. Rev.108.1645 (1957)

$$\mathbf{P}_\Lambda^* = \frac{(\alpha_\Xi + \mathbf{P}_\Xi^* \cdot \hat{p}_\Lambda^*)\hat{p}_\Lambda^* + \beta_\Xi \mathbf{P}_\Xi^* \times \hat{p}_\Lambda^* + \gamma_\Xi \hat{p}_\Lambda^* \times (\mathbf{P}_\Xi^* \times \hat{p}_\Lambda^*)}{1 + \alpha_\Xi \mathbf{P}_\Xi^* \cdot \hat{p}_\Lambda^*}$$

$$\alpha^2 + \beta^2 + \gamma^2 = 1$$

$$\mathbf{P}_\Lambda^* = C_{\Xi^-\Lambda}\mathbf{P}_\Xi^* = \tfrac{1}{3}\left(1 + 2\gamma_\Xi\right)\mathbf{P}_\Xi^*.$$

$$C_{\Xi^-\Lambda} = +0.944$$

spin 3/2

Similarly, daughter Λ polarization from Ω:

$$\mathbf{P}_\Lambda^* = C_{\Omega^-\Lambda}\mathbf{P}_\Omega^* = \tfrac{1}{5}\left(1 + 4\gamma_\Omega\right)\mathbf{P}_\Omega^*.$$

Here **γ_Ω is unknown**.

- Time-reversal violation parameter β_Ω would be small
- α_Ω is very small

then $\gamma_\Omega \sim \pm 1$ and the polarization transfer $C_{\Omega\Lambda}$ leads to:

$$C_{\Omega\Lambda} \approx +1 \text{ or } -0.6$$

Parent particle polarization can be studied by measuring daughter particle polarization!

Polarization of vector mesons: $K^*(892)$ and ϕ

Non-central heavy-ion collisions:

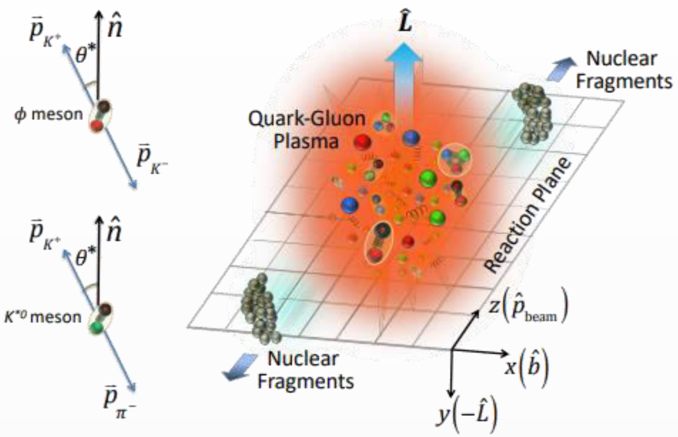

$$\frac{dN}{dcos\theta} = N_0[1 - \rho_{0,0} + cos^2\theta(3\rho_{0,0} - 1)]$$

$\rho_{0,0}$ is a probability for vector meson to be in spin state = 0 → $\rho_{0,0}$ = 1/3 corresponds to no spin alignment

The large ρ_{00} puzzle

$$\rho_{00} \approx \frac{1}{3} + C_\Lambda + C_\varepsilon + C_E + C_F + C_L + C_A + C_\varphi + C_g$$

Physics Mechanisms	(ρ_{00})
c_Λ: Quark coalescence vorticity & magnetic field[1]	< 1/3 (Negative ~ 10^{-5})
c_ε: E-comp. of Vorticity tensor[1]	< 1/3 (Negative ~ 10^{-4})
c_E: Electric field[2]	> 1/3 (Positive ~ 10^{-5})
c_F: Fragmentation[3]	> or, < 1/3 (~ 10^{-5})
c_L: Local spin alignments[4]	< 1/3
c_A: Turbulent color field[5]	< 1/3
c_φ: Vector meson strong force field[6]	> 1/3 (Can accommodate large positive signal)
c_g: Glasma fields + effective potential	could be significant

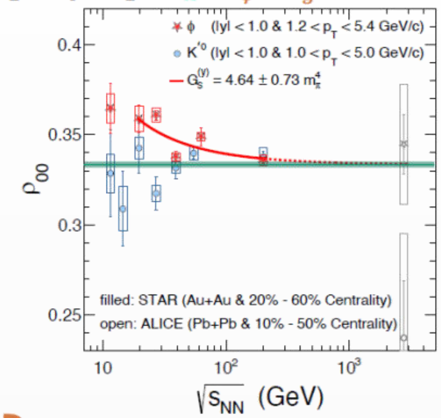

STAR, Nature 614 244 (2023)

strong force

Nature 614 244 (2023)

ϕ exhibits surprisingly large global spin alignment while K* displays little.

Aihong Tang. QuarkMatter 2023, Houston, Sept 3-9 18

- Measurements at RHIC/LHC challenge theoretical understanding → ρ_{00} can depend on multiple physics mechanisms (vorticity, magnetic field, hadronization scenarios, lifetimes and masses of the particles …)
- Measurements should be extended to lower collision energies

Critical fluctuations

- Ratio of the 4th-to2nd moment of the (net)proton multiplicity distribution:
  - ✓ non-monotonic behavior → deviation from non-critical dynamic baseline close to CEP ???

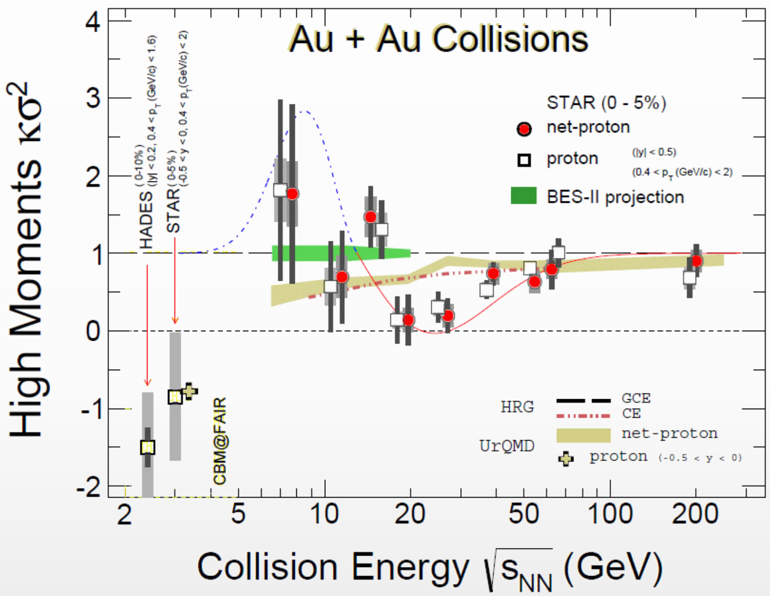

- Interpretation of results requires understanding of the role of finite-size effects, which have specific dependence on the size and duration of formed system

Significant <u>improvement of statistical precision and systematic</u> uncertainties and <u>extra points</u> in the NICA energy range are required